UNIVERSITÀ DEGLI STUDI DI GENOVA

GENUENSE ATHENAEUM

SCUOLA DI SCIENZE MEDICHE E FARMACEUTICHE

DIPARTIMENTO DI NEUROSCIENZE, RIABILITAZIONE, OFTALMOLOGIA, GENETICA E

SCIENZE MATERNO-INFANTILI

DOTTORATO DI RICERCA in SCIENZE PEDIATRICHE

CURRICULUM PATOLOGIA FETO-PERINATALE E PEDIATRICA (XXXVIII CICLO)

TESI DI DOTTORATO

Improving Metabolic Stability in Preterm Infants Using Continuous Glucose Monitoring: A Randomized Study

Relatore

Prof. Luca Antonio Ramenghi

Candidato

Dott.ssa Marcella Battaglini

Direttore Corso di Dottorato

Prof Pasquale Striano

ABSTRACT

Background: preterm infants are particularly vulnerable to glycaemic instability, a condition associated with increased neonatal morbidity and adverse neurodevelopmental outcomes. Continuous glucose monitoring (CGM) has emerged as a promising tool for improving metabolic management by enabling continuous assessment of glucose fluctuations. This study aimed to evaluate whether real-time CGM improves glycaemic control and influences brain development and neurodevelopmental outcomes compared with standard intermittent glucose monitoring in very preterm infants.

Methods: a single-centre prospective randomized controlled trial was conducted in a tertiary Neonatal Intensive Care Unit between January 2022 and August 2023. Preterm infants were randomized within six hours of birth to either real-time CGM-guided management or standard care with blinded CGM. Glycaemic management in the intervention group was adjusted according to continuous real-time glucose trends, whereas treatment decisions in the control group relied on intermittent blood glucose measurements. Primary outcomes included frequency and duration of hypoglycaemic (<47 mg/dL) and hyperglycaemic (>180 mg/dL) episodes. Secondary outcomes comprised assessment of glycaemic variability using the Mean Amplitude of Glycaemic Excursions (MAGE), evaluation of white matter microstructural maturation through tract-based spatial statistics (TBSS) at 33 weeks postmenstrual age and at term-equivalent age, and neurodevelopmental assessment at two years corrected age using the Griffiths Scales of Child Development.

Results: fifty-three infants were enrolled (real-time CGM: n=26; control: n=27). Infants monitored with real-time CGM showed a significant reduction in both hypoglycaemic and hyperglycaemic episodes during the first week of life and at 32 weeks postmenstrual

age. Despite improved metabolic stability, no significant differences were observed in white matter microstructure or neurodevelopmental outcomes at two years corrected age. **Conclusions**: real-time CGM significantly improves metabolic stability in very preterm infants by reducing dysglycaemic episodes and glycaemic variability, factors potentially relevant for neuroprotection. The absence of detectable neurodevelopmental differences may reflect limited statistical power or the multifactorial nature of preterm brain injury. Larger multicentre studies are warranted to clarify the long-term neurological impact of CGM-guided metabolic management and to support the development of evidence-based neonatal glucose control strategies.

ABBREVIATIONS

ADC apparent diffusion coefficient

AD Axial diffusivity

CBH Cerebellar Haemorrhage

CGM Continuous Glucose Monitoring

DTI Diffusion Tensor Imaging

DWI Diffusion Weighted Imaging

EEG Electroencephalography

ELBW Extremely Low Birth Weight

EUGR Extra Uterine Growth Resstriction

FA Fractional anisotropy

GM Grey matter

GMDS Griffiths Scales of Child Development

GV Glycaemic Variability

IUGR Intrauterine Growth Restriction

IVH Intraventricular Haemorrhage

LGA Large for Gestational Age

MAG Mean Absolute Glucose

MAGE Mean Amplitude of Glycaemic Excursions

MD Mean Diffusivity

MEG Magnetoencephalography

MRI Magnetic Resonance Imaging

NICU Neonatal Intensive Care Unit

PLIC Posterior Limb of the Internal Capsule

PTB Preterm birth

ST Standard Deviation

SWI susceptibility-weighted imaging

RD Radial diffusivity

ROI Region of interest

ROS Reactive Oxygen Species

RT-CGMs Real Time Continuous Glucose Monitoring

TBSS Tract-Based Spatial Statistics

VLBW Very Low Birth Weight

WM White matter

VBM Voxel-Based Morphometry

INTRODUCTION

Preterm birth (PTB) is defined as any live birth occurring before 37 completed weeks of gestation; this can be subdivided into extremely preterm (<28 weeks), very preterm (28–<32 weeks), moderately preterm (32–<34 weeks) and late preterm (34–<37 weeks) birth based on the gestational age at delivery [1].

This subcategorization is important because gestational age is inversely associated with increased mortality, morbidity and the intensity of neonatal care required at birth [2].

Worldwide, 11.1% of infants are born preterm every year. PTB is the leading cause of perinatal morbidity and mortality and second most common cause of death, after pneumonia, in children under 5 years of age [3].

1 Hypoglycaemia in newborn

The definition of hypoglycaemia in the newborn infant has remained controversial because of lack of significant correlation between plasma glucose concentration, clinical symptoms, and long-term sequelae [4,5]. As we know glucose is the main fuel for central nervous system metabolism, so persistence of an inadequate blood value can lead to irreversible neurological damages [6].

Hypoglycaemia is a common metabolic problem in newborns caused by a difficulty to control glucose metabolism. Glucose is the primary source of energy for the growing foetus.

At the exact moment of cord clamping there is an immediate cessation of maternal oxygen and nutrient support. From this instant, the infant must spontaneously provide for its own glucose homeostasis [4].

In the first hour of life there is a rapid decline in glucose concentration followed by an increase that occurs within 2-3 hours of the newborn. Hepatic glycogenolysis is the fastest mechanism increasing blood glucose levels after birth. The high rate of glycogenolysis leads to depletion of hepatic glycogen stores, especially in preterm infants in which liver glycogen deposits are limited. Gluconeogenesis is not immediately effective after birth due to the initial low enzymatic activity of this pathway. Gluconeogenesis slowly starts after some hours from birth and reaches its maturation after 12 h [7]. Glucose oxidation supports about 70% of the energy requirement of the brain. Ketone bodies and lactate are important alternative fuels to reduce the glucose requirement. Hepatic ketogenesis markedly increases during the first hours from birth, to provide alternative fuels for brain metabolism in term infants. However, this metabolic pattern is severely limited in preterm infants due to a lack of fat stores in adipose tissue, which eventually results in failure of lipolysis [8] [Figure 1].

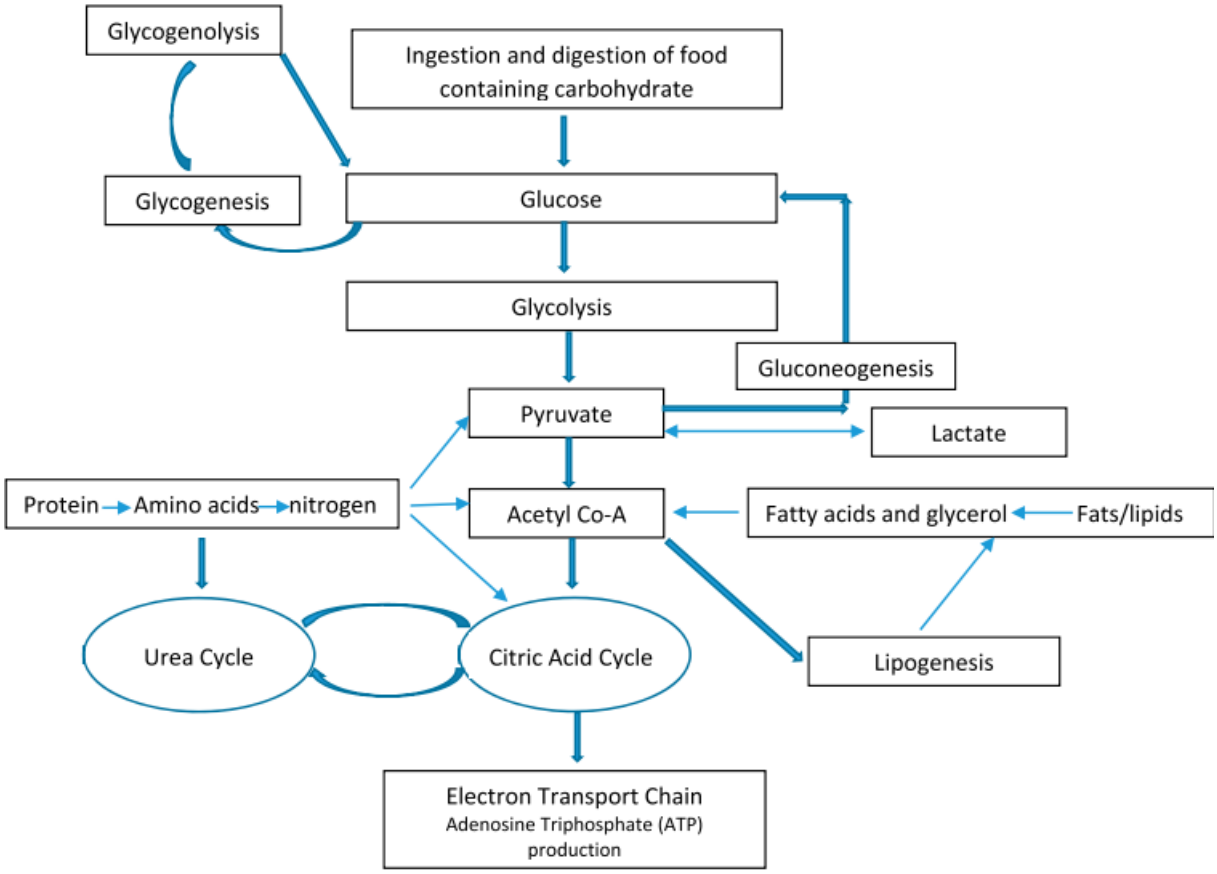

Figure 1. Glucose homeostasis

Hypoglycaemia occurs in an infant who is born with low glycogen and fat stores, with limited capacity to generate glucose via the gluconeogenesis pathway or, when, there is an excessive peripheral tissue utilization of glucose like in an infant of a mother with insulin dependent diabetes or a large for gestational age newborn (LGA) [9].

Most studies have shown that premature infants are more vulnerable than full-term infants to remain normoglycemic in the first week of life. This depends on several mechanisms. Predisposition to hypoglycaemia could be due to low glucose-6-phosphatase activity, the existence of an incompletely coordinated counter-regulatory system, increased basal metabolism of glucose, a lower capacity for production of alternative energy sources and presence of clinical conditions associated with hypoglycaemia, such as perinatal asphyxia, hypoxia, sepsis, and hypothermia[10]. Consequently, it is essential to provide exogenous glucose at birth, especially in preterm infants [11].

The definition of hypoglycaemia is controversial[12]. Neonatal hypoglycaemia is defined as a blood glucose concentration of less than 47 mg/dL (2.6 mmol/L). According to the American Academy of Paediatrics, asymptomatic blood glucose concentrations of less than 25 mg/dL (1.4 mmol/L) within 2 hours of birth in healthy term neonates do not require treatment, as this is part of a glucidic adaptation from intrauterine to extrauterine life. Intravenous glucose administration is only recommended if blood glucose levels fall below 25 mg/dL (1.4 mmol/L) within the first 4 hours, or below 35 mg/dL (2.0 mmol/L) between 4 and 24 hours after birth [13]. In term newborns, the estimated incidence of symptomatic hypoglycaemia is 1–3/1000 live births.

1.1 Hypoglycaemia and hyperglycaemia in preterm babies

Preterm infants have a threefold higher incidence of symptomatic hypoglycaemia, known to be associated with cerebral damage [6]. Preterm infant hypoglycaemia is caused by low glucose-6-phosphatase activity, insufficient glycogen stores, and a limited capacity to access alternative energy sources [7,10].

Hyperglycaemia, hypoglycaemia, and glycaemic instability are common in preterm infants and have been associated with increased risk of mortality and morbidity. Hyperglycaemia, defined as blood glucose levels greater than 10 mmol/L (180 mg/dL), is also common in extremely preterm infants [14]. In very-low-birth weight (VLBW, <1500 g) infants, especially those born small for gestational age, the incidence of hyperglycaemia is high (20 to 86%). The pathogenesis of hyperglycaemia in VLBW infants is complex: intracellular glucose deprivation, a consequence of low postnatal insulin levels, may initiate counterregulatory responses and catabolism, leading to hyperglycaemia [15].

Hyperglycaemia is indirectly related to birth weight and gestational age and is directly related to illness, to treatment with corticosteroids, and to intravenous glucose infusions given at rates exceeding normal infant glucose turnover rates. Hyperglycaemia in very sick patients is most likely an effect of stress and thus increased levels of catecholamines, which are known to stimulate glucose metabolism. However, the glucose intolerance observed in healthy, premature infants receiving glucose infusions at rates exceeding their normal glucose turnover rate is specifically related to their immaturity and might be a result of absolute or relative insulin insufficiency, hepatic and peripheral insulin resistance, inadequate responsiveness to insulin and/or glucose, and the small mass of insulin-dependent tissue (muscle and fat) [16].

Hyperglycaemia can lead to acute problems of osmotic diuresis and metabolic acidosis and has been associated with increased risk of intraventricular haemorrhage, patent ductus arteriosus, retinopathy of prematurity, necrotising enterocolitis, and a reduction in white matter maturation [16]. Attempts to reduce risks associated with hyperglycaemia can increase the risk of hypoglycaemia, which has been associated with poor developmental outcomes.

Consequently, therapeutic changes are extremely important in the first days of life, as on the one hand the infant needs energy to grow adequately, but on the other hand sudden changes in insulin sensitivity put him at risk of both hypoglycaemia and hyperglycaemia [17].

1.2 Clinical manifestations in infancy

A rapid decline in blood glucose concentration activates an autonomic response and causes neuroglycopenia, which may lead to neurological dysfunction. In newborns, the signs of hypoglycaemia are more subtle and too often asymptomatic [18]

If present, the symptoms in newborns include cyanosis, pallor, apnoeic episodes, tachypnoea, hypothermia, hypotonia, poor feeding, abnormal cry (weak or high- pitched), irritability, diaphoresis, tremors, jitteriness, exaggerated Moro reflex, lethargy and seizures. Most of these signs are not specific to hypoglycaemia and can also be manifestations of other neonatal disorders (septicaemia, congenital heart disease, ventricular haemorrhage and respiratory distress syndrome).

Neonatal hyperglycaemia is also mostly asymptomatic and possible signs are also indicative of other pathological processes [19]. The symptoms include dehydration due to osmotic diuresis, weight loss, failure to thrive, fever, glucosuria, ketosis and metabolic

acidosis. In the newborn, especially if preterm, signs and symptoms of glucose imbalance are infrequent and when present are indicative of important alterations [Figure 2].

Neurogenic (Autonomic activation of the sympathetic nervous system)	Neuroglycopenic (Central nervous system deprivation of glucose supply)
Pallor	Weak or high-pitched cry
Jitteriness	Apnea
Tremors	Hypotonia
Tachypnea	Seizures
Sweating	Lethargy
Irritability	Coma
Tremulousness	
Vomiting	
Temperature instability	
Tachycardia	
Exaggerated Moro reflex	

Figure 2. Symptoms of hypoglycaemia in newborn

1.3 Neonatal hypoglycaemia and brain vulnerability

Hypoglycaemia causes neuronal depolarization, resulting in a significant increase in brain glutamate concentrations. Impaired glutamate reuptake results in aspartate accumulation in brain tissues. Consequently, increased levels of aspartate may activate some glutamate receptors subtypes, contributing to excitotoxicity. The sustained glutamate receptor activation is the first step of the process leading to neuronal cell death [20].

The oxidative DNA damage is the second major player in cellular death: mitochondria taken from a hypoglycaemic brain show a great capacity to generate reactive oxygen species (ROS) in response to glutamate excitotoxicity. However, ROS can also be generated by several other sources. NADPH oxidase is an enzyme which synthesizes superoxides. It has been observed that superoxide production in neuron cells affected by hypoglycaemia occurs mainly during glucose reperfusion [21].

Zinc (as Zn2+) is a neuromodulator stored within vesicles in presynaptic terminals, and it is massively released from into the extracellular space during pathological conditions such as ischemia, seizure, brain trauma, and hypoglycaemia. Zinc significantly affects the activity of many receptors, and it has been associated with the promotion of neuronal death. It induces mitochondrial dysfunction triggering mitochondrial depolarization and leading to PARP-1 activation, because of increased production of reactive oxygen species (ROS) [22].

PARP-1 facilitates the DNA repair process. During oxidative stress, reactive species damage all cellular components, including nucleic acids. PARP-1 activation helps the DNA repair machinery. While adequate PARP activation facilitates DNA repair, extensive PARP activation, caused by extensive damage from a sustained action of glutamate, induces mitochondrial permeability transition and mitochondrial damage that culminates in cell death [6,23].

The selective vulnerability of brain regions to hypoglycaemia has been demonstrated. The II and III superficial layers of the cerebral cortex, the dentate gyrus, the subiculum, the CA1 regions in the hippocampus, and the caudate - putamen, are the main susceptible areas to hypoglycaemic insult. Although the physiopathology underlying this different susceptibility is still unclear, oxidative stress seems to play a central role [24].

Another controversial topic is whether the extent of lesions found on Magnetic Resonance Imaging (MRI) and long-term outcome can be correlated. Occipital lobe damage is the predominant one. As we can observe from the images below, the occipital lobe injury can be evident in the acute phase on the diffusion-weighted imaging (DWI) [Figure 3].

Occipital cortex damage is associated with visual deficits and epilepsy of occipital origin. The outcomes depend greatly on the duration of the hypoglycaemic event and its severity.

MRI that was performed promptly after insult could be of help in predicting visual outcomes, although, as mentioned earlier, it is not always easy to correlate the extent of damage with long-term outcomes [25].

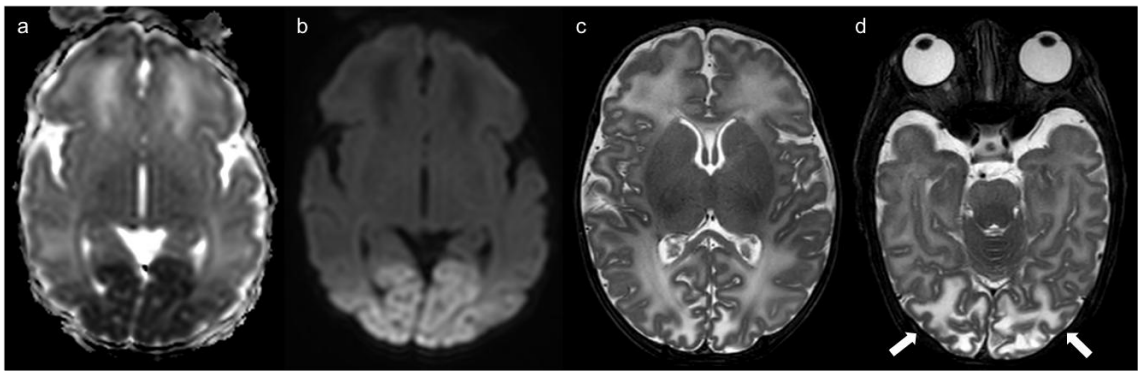

Figure 3. Hypoglycemia occipital cortex damage in a newborn. At birth damage manifests as restriction in (a) ADC maps and (b) DWI b1000 imaging. At 1 month of age is visible in T2-weighted imaging (c-d).

2 The brain vulnerability of the preterm infant and the role of MRI in predicting brain maturation

Brain vulnerability changes with gestational age and depends on the characteristics and stages of brain development [26].

The brain of an extremely preterm infant is characterised by significant developmental changes that are especially noticeable in the cerebellum and in the periventricular zone, both of which host evolving germinal matrix, which is a common site of injury in the preterm.

It is vulnerable to rupture and haemorrhage due to the poor vascular integrity of involuting immature vessels and inadequate connective tissue support with a deficiency in mesenchymal and glial elements. These intrinsic characteristics of the germinative matrix increase its vulnerability and the risk of bleeding. Impaired cerebrovascular

autoregulation with frequent fluctuations in carbon oxide, disturbances in coagulation, large patent ductus arteriosus and other parameters further exacerbate this danger [27].

The vulnerability of the brain between 26 and 34 weeks of postmenstrual age is mainly connected to the white matter development, especially in the periventricular zones [28].

This vulnerability appears to be multifactorial, relating to vessel anatomy with regions of relatively poor perfusion, low baseline blood flow, impaired regulation of blood flow and the inherent susceptibility of pre-oligodendrocytes to damage [29].

The usefulness of MRI at term equivalent age is well known. It can give information about the asymmetry of the PLIC (posterior limb of the internal capsule), a predictor of hemiplegia. A bilateral abnormal signal intensity of the PLIC could be an early predictor of spastic diplegia or quadriplegia [30].

Assessment of myelination at the level of the PLIC is considered the simplest and most useful way to evaluate the normal development of myelination in term babies and in preterm babies at term corrected age [26].

Together with brain maturation assessed through morphological analysis of brain lesions, a further method to analyse brain maturation is Diffusion Tensor Imaging (DTI) studies. These studies allow to identify those microstructural abnormalities in the developing white matter aiming to predict and follow the changing neurological problems of ex-preterm babies, not anymore characterised by severe disabling handicaps, but more focused on psychological and behavioural problems [31].

2.1 Neuroimaging Techniques in the Study of the Preterm Newborn

Neuroimaging techniques are increasingly used in clinical practice to assess, plan treatment, and formulate a prognosis in newborns. Over the last forty years, both standard

and advanced technologies have undergone rapid development, resulting in a significant increase in diagnostic capabilities and quality of clinical information. With these advances, the use of imaging techniques in the neonatal population has become an established routine in both daily clinical practice and scientific research. These tools not only allow for an accurate assessment of neonatal neurophysiology but also promote a deeper understanding of the pathophysiology of neurological diseases in the neonatal period. Moreover, they play an essential role in the development and validation of new therapeutic strategies, thereby contributing to improved treatments and, consequently, better clinical outcomes.

MRI is the most sensitive technique among those available. It provides high-definition images of central nervous system structures and offers the advantage, compared with CT, of avoiding ionizing radiation[32,33]. However, it also has some limitations, including high cost, reduced availability, and the need for complete immobilization of the newborn during the examination, which may require sedation or non-pharmacological immobilization strategies[34].

2.2 Magnetic Resonance Imaging (MRI)

To date, magnetic resonance imaging (MRI) represents the most advanced modality in diagnostic neuroimaging, serving as a cornerstone for the evaluation and characterization of brain structures under both physiological and pathological conditions. Owing to its capacity to generate high-resolution, three-dimensional images in a non-invasive manner, MRI has become an indispensable tool in neuroradiology. It not only enables precise diagnosis of neurological disorders but also provides critical insight into the pathophysiological mechanisms that underlie different clinical conditions[35]. When MRI-

derived metrics are integrated with clinical, behavioral, and electrophysiological markers, they allow for early diagnosis and prognostic stratification, ultimately supporting timely interventions that may mitigate long-term neurodevelopmental disability in children[36].

MRI also enables the visualization and quantification of the human brain's developmental trajectory, which begins in the fetal period and continues throughout childhood. Across this interval, key neurobiological processes, including neuronal migration, myelination, and synaptogenesis, occur in a highly regulated temporal sequence, each essential for the establishment of long-term cerebral function[37].

Among these processes, myelination is particularly critical because it enhances the efficiency and velocity of action potential conduction. This process does not unfold uniformly across the brain but follows a caudo–rostral gradient, initiating in posterior regions and subsequently progressing anteriorly. Preterm birth disrupts this spatial–temporal pattern, and the degree of disruption is closely associated with gestational age[37]. These microstructural transformations underline the evolving MRI signal characteristics observed during normal brain maturation. In neonates, T1- and T2-weighted signal intensities in white matter (WM) and gray matter (GM) appear essentially "inverted" relative to the adult brain[38]. Over the first two years of life, T1 and T2 relaxation times decreased rapidly and continuously, with more pronounced changes in WM than in GM. This evolution reflects progressive alterations in myelin composition and organization[38]. Specifically, the increase in T1 signal within WM is largely attributable to interactions between water and myelin-associated macromolecules (including cholesterol, glycolipids, and structural proteins), whereas the reduction in T2 signal corresponds to shifts in tissue hydration and increased compaction of the myelin sheath[39]. As myelination advances, signal characteristics converge toward the adult pattern, reaching near-adult appearance by approximately 12 months on T1-weighted images and between 24 and 30

months on T2-weighted images. These changes reflect the structural and functional maturation that supports more efficient neural transmission and contributes to the stabilization of cognitive and sensorimotor functions[39].

Collectively, these factors account for the widespread adoption and growing clinical relevance of MRI, both for the characterization of neurological disorders and for longitudinal monitoring of brain development[40].

2.3 DWI e DTI

Alterations in neonatal blood glucose levels—whether hyperglycemia or hypoglycemia—can induce brain injury and impair neuronal development. Functional disturbances related to these metabolic abnormalities can be investigated using several neurophysiological techniques, including high-density electroencephalography (EEG) and non-invasive magnetoencephalography (MEG), which allow for the assessment of neuronal connectivity. However, these modalities do not provide the same degree of specificity and sensitivity as diffusion-weighted MRI (Diffusion Weighted Imaging, DWI), a technique that is now extensively validated in clinical practice[41].

DWI enables the detection of microstructural changes within cerebral WM, revealing functional abnormalities even in the absence of evident structural lesions[42]. This MRI sequence measures the displacement of water molecules within tissues according to Brownian motion[43]. Water diffusion may occur isotropically, without directional constraints, as in cerebrospinal fluid, or anisotropically, with preferential displacement along a specific axis, as observed in myelinated WM. By varying the degree of diffusion weighting, it is possible to generate apparent diffusion coefficient (ADC) maps, which quantify the speed and amplitude of molecular motion[44].

Acquiring DWI data along multiple gradient directions yield diffusion tensor imaging (DTI), which computes a diffusion tensor for each voxel and thereby characterizes the three-dimensional orientation of neural fibers[45]. This approach is widely used to study the developing brain. The fundamental principle of DTI is that water diffusion reflects tissue microstructure, including cell type, structural integrity, presence of microstructural barriers, and axonal packing density[46]. As such, DTI provides quantitative information on diffusion orientation and anisotropy, which is essential for investigating both normal and abnormal neurodevelopment.

The diffusion tensor is represented by a 3×3 matrix containing six independent parameters[47]. Its computation requires at least six non-collinear diffusion directions in addition to one non-diffusion-weighted (b=0) image; however, higher angular sampling (≥32 directions) yields improved reconstruction accuracy[48]. The tensor can be decomposed into eigenvalues (λ_1, λ_2, λ_3), which describe the magnitude of diffusion along the principal axes, and eigenvectors (ε_1, ε_2, ε_3), which represent their orthogonal directions. Graphically, diffusion may be visualized as a three-dimensional ellipsoid[49].

Several quantitative metrics can be derived from DTI, including:

- **Axial diffusivity (AD):** diffusion parallel to the main fiber axis;
- **Radial diffusivity (RD):** diffusion perpendicular to the fibers;
- **Mean diffusivity (MD):** an overall measure of molecular mobility;
- **Fractional anisotropy (FA):** ranges from 0 (free diffusion) to 1 (fully directional)[50].

FA maps can be color-coded, with red indicating left–right diffusion, green indicating anteroposterior diffusion, and blue reflecting craniocaudal orientation[51].

In WM, diffusion is anisotropic due to the longitudinal arrangement of axons, which restricts transverse water displacement. In GM, which is less structurally organized, diffusion is less anisotropic, whereas in CSF it is fully isotropic[52]. During myelination, an increase in FA and AD is typically observed, accompanied by reductions in RD and MD. Conversely, reductions in FA and AD together with increases in RD and MD may indicate axonal injury[45].

Despite the value of DTI for in vivo investigation of the neonatal brain, several physiological and technical limitations must be considered. Physiologically, in early development, image quality may be reduced by low myelin content, similar water content between WM and GM, and limited axonal organization[53–55]. From a technical point of view, it is essential to ensure adequate signal-to-noise ratio and sufficient spatial and

contrast resolution[53]. Major artifacts that can compromise DTI data include spontaneous, respiratory, or cardiac motion, which can be mitigated using single-shot echo-planar imaging (EPI)[52,56], magnetic susceptibility artifacts causing signal loss or distortion[57], which can be partially corrected with dedicated algorithms[58–60] and instrumental factors such as low ambient humidity.

2.4 Post-analysis of DTI

Once metrics derived from diffusion-weighted imaging have been collected, they can be subjected to analysis using several methodologies, which allow for a detailed and targeted study of cerebral white matter. The available methodological options for data processing and interpretation of DTI images can be divided into: region of interest (ROI) analysis and tract-based spatial statistics (TBSS)[45].

ROI analysis consists of isolating a specific brain region for further investigation. This is a defined portion of the image, manually selected based on anatomical criteria, on which diffusion parameters (particularly FA and MD) are calculated to perform localized quantification[61]. This methodology, however, is time-consuming and heavily dependent on the operator's anatomical and radiological knowledge.

The most recent method, which attempts to overcome these criticalities, is TBSS. This is an automated, voxel-wise analysis that detects diffuse microstructural differences in white matter between groups of subjects. The basic principle involves creating a "mean FA skeleton," which represents the centers of major fiber tracts common to all participants. This process reduces misalignment errors and improves spatial correspondence between subjects[62]. TBSS does not require spatial smoothing, increases statistical power by reducing the number of tested voxels, and improves the objectivity

and interpretability of results[63]. Furthermore, it is less influenced by factors such as cerebral atrophy, imprecision in tract tracing, and partial volume effects[63].

For all these reasons, DTI associated with TBSS currently represents an extremely useful tool for the in vivo study of cerebral microstructures, as it provides detailed and quantitative measurements directly associated with both brain lesions and neurodevelopmental processes.

3 Continuous glucose monitoring (CGM)

Strict monitoring of glucose levels is necessary to prevent and treat glucose imbalances. Although serum glucose measurement is considered the gold standard in infants, glucose monitoring depends on intermittent heel pricks and frequently repeated sampling.

This method has some limitations: low glucose concentration might not be detected by intermittent blood glucose monitoring and conversely blood glucose concentration may be assessed when the infant is only temporary hypoglycaemic, leading to unnecessary treatment. Further, serial blood glucose monitoring by heel lancing is invasive, with potential adverse effects on neurodevelopment [64].

Continuous glucose monitoring (CGM) has the advantage of tracking glucose levels continuously and thus providing a reliable glycaemic profile of patients [65]. While CGM is well established in the management of diabetes mellitus, its role in neonatal glycaemic control is more controversial.

CGM offers the possibility of adjusting treatment in real time to account for individual metabolic requirements while reducing the number of blood glucose measurements and potentially improving long-term outcomes [66]. The clinical interpretation of CGM is challenging and in the absence of well-established guidelines, there is a risk that CGM

could lead to unnecessary or even harmful intervention [67]. Finally, CGM is less accurate than heel pricks because it needs to be interpreted as a dynamic and integrated value than as a static number as in the case of glucometers.

There are several types of CGM devices, interstitial, subcutaneous or transdermal. Among the subcutaneous, there are microdialysis fibres and amperometric needle electrodes; the latter are the commercial devices currently used in newborn [Figure 4].

These consist of a fine needle sensor connected to a non-implantable transmitter that powers the sensor and sends raw data to a monitor, either by cable or Bluetooth. The system displays the resulting output in "real time" on the monitor. Amperometric sensors measure current flowing from an oxidation (electron producing) reaction at a working electrode to a reduction (electron consuming) reaction at a counter electrode. The working electrode is coated with glucose oxidase which catalyses the oxidation of glucose when a voltage is applied, resulting in transfer of electrons to a chemical mediator, usually hydrogen peroxide. A reference electrode is used to ensure a stable voltage applied to the working electrode, but reference and counter electrodes are often combined. In addition, subcutaneous sensors require a barrier membrane to limit glucose access to the sensor because of the deficiency of oxygen in the subcutaneous environment relative to glucose supply. Each manufacturer has their own proprietary method for combining these elements within the needle sensor [68].

Raw signal data from the electrode is generated approximately every 10 seconds and is averaged and processed to give a glucose reading every 5 minutes, thus providing near continuous output [68]. Blood glucose concentration is estimated from this signal using proprietary algorithms based on regular calibration to blood glucose measurements (minimum 12 hourly). One limitation is that sensors require a "calibrating phase" at the

beginning, which is typically around two hours, for stabilization of signal output. This results in 2 hours wait to obtain the first glucose value.

Despite some limitations, real-time CGM may help to achieve greater glucose stability in newborns, particularly in preterm babies.

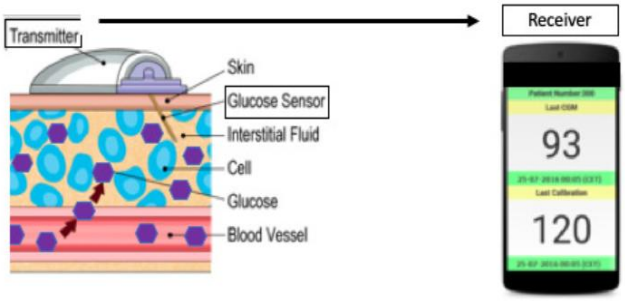

Figure 4. Continuous glucose monitoring: overview of the main sensor components

3.1 Glycaemic variability (GV)

Glucose metabolism is influenced by many factors and, in common with other physiological processes, is characterized by constant fluctuations. In addition to hypoglycaemia and hyperglycaemia, the global picture of glucose metabolism involves a third measurement called GV, which has attracted much interest in recent years. In adults with type 2 diabetes, it was demonstrated that rapid blood glucose fluctuations have more specific triggering effects on oxidative stress than chronic sustained hyperglycaemia alone [69]. On the other hands, oxidative stress has been shown to be significant in the pathogenesis of numerous neonatal diseases, including periventricular leukomalacia, bronchopulmonary dysplasia, and retinopathy of prematurity [70].

It has been shown that increased glycaemic variability relates to oxidative stress, which results in direct cellular damage and apoptosis.

The relationship between GV and mortality was reported in VLBW infants and term neonates, but not always CGM was used [71].

Glycaemic variability is a complex phenomenon that includes both intraday and interday variability. This concept is mostly concerning the diabetic subjects, both adults and children, and literature is dedicated to this population. There are only few studies about GV in neonates and mostly have been carried out among preterm infants [72,73].

Standard Deviation (SD) around a mean glucose value measured over a 24 h period using the CGM is probably one of the most appropriate tools for assessing intraday glycaemic variability [74].

The intraday component corresponds to the within-day vertical glycaemic fluctuations, while the interday component is defined as day-to-day glucose variations, i.e., glycaemic variability along a time-dependent horizontal axis. Such a method integrates both minor and major fluctuations but does not permit differentiation of the major from the minor

ones. The other methods developed for estimating the intraday glycaemic variability are based on the determination of differences between maximum and minimum glucose levels. In particular, the Mean Amplitude of Glycaemic Excursions (MAGE) [Figure 5] index is probably more appropriate for selecting the major glucose swings that are calculated as the arithmetic mean of differences between consecutive peaks and nadirs, provided that the differences be greater than the SD around the mean values. Calculating the MAGE index requires continuous glucose monitoring, which has the advantage to detect all isolated upward and downward acute glucose fluctuations. The MAGE remains certainly the most comprehensive index for assessing the intraday glycaemic variability, it has two main advantages: first, this parameter is not dependent on the mean glucose value, and second, it is designed to quantitate major glucose swings and exclude minor ones.

Figure 5. Example of MAGE calculation, cited by Characterizing Blood Glucose Variability Using New Metrics with Continuous Glucose Monitoring Data, Journal of Diabetes Science and Technology, 2011

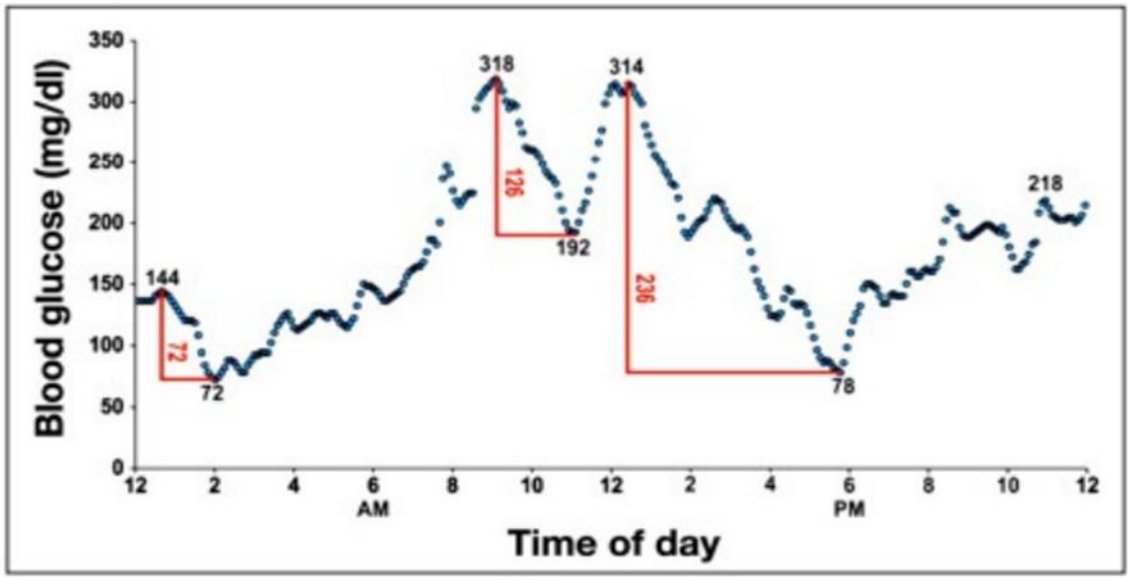

The Mean Absolute Glucose (MAG) index is the summed differences between sequential 7-point self-measured blood glucose profiles per 24 h divided by the time in hours

between the first and last blood glucose measurement. A limitation to MAG is that two excursions of identical extent but of different duration have different values [Figure 6].

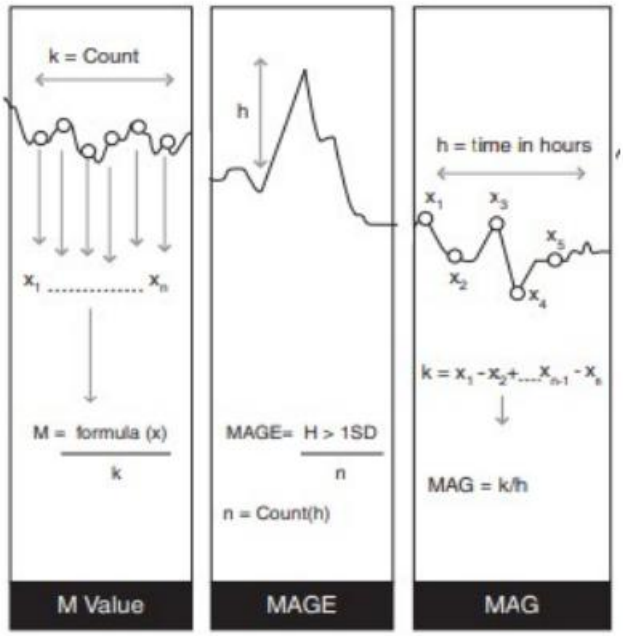

Figure 6. Graphical rapresentation of variability index

4 PURPOSE OF THE STUDY

4.1 Primary objective:

The main objective of the study is to evaluate if continuous glycemic monitoring in preterm babies allows to maintain euglycemia for a longer time compared to patients treated with standard of care.

4.2 Secondary objectives:

1. To compare the two groups in terms of glycaemic variability, investigating whether continuous glycaemic monitoring can result in reduced glycaemic variability.
2. To evaluate the effect of CGM on cerebral white matter development in preterm neonates, as compared with standard-of-care glycemic management, by means of TBSS analysis, to detect significant differences in cerebral white matter microstructure.
3. To evaluate inter-group differences in psychomotor development at 24 months of corrected age through the administration of the Griffiths Mental Development Scales.

5 MATERIALS AND METHODS

5.1 Patients

This is a single-centre, prospective, pilot, and interventional study performed in neonatal intensive care unit (NICU) of Giannina Gaslini Institute (Genoa) from January 2022 to August 2023.

Premature infants with a gestational age between 26+0 and 31+0 weeks and a birth weight > 800 g were enrolled in the study. Recruitment was among patients born at the Obstetrics Department of the Giannina Gaslini Institute.

During the informational interview with the Family, the purpose of the study and the procedures involved in case of child's participation were described.

After informed consent was obtained, each infant was assigned an identification number and put into a database to collect the patient's general information at birth and during hospitalization.

All preterm infants enrolled were treated according to the standard of care appropriate for gestational age and birth weight.

Specifically, an umbilical venous catheter was placed within the first hour of life to ensure proper glucose supply that could not be administered enterally or through peripheral venous access. The initial glucose infusion rate was defined by the physician in accordance with the ESPGHAN 2018 guidelines [11]. The glycaemic rate is often between 4 and 5 mg/kg/min and then increased or decreased according to the infant's glucose need.

5.2 Eligibility criteria

a) Inclusion criteria

- Newborn with gestational age between 26+0 and 31+0 and with a weight above 800 g.
- Patients born at the Obstetrics Department of the Giannina Gaslini Institute.
- Informed consent dated and signed by parents.
- Adult parents

b) Exclusion criteria

- Newborn with genetic diseases or chromosomal abnormalities.
- Newborn whose parents have not given consent for participation in the study.

Furthermore, the inclusion criteria for the neuroimaging analysis were defined as availability of DTI and T2-weighted images acquired on a 3T scanner around the 33rd week, as well as corrected term-equivalent age. Whereas the exclusion criteria were the presence or diagnosis of other comorbidities that could impact white matter development, such as GMH-IVH or NEC.

5.3 Randomization

Patients were randomized into two groups with an allocation ratio 1:1. They were randomly assigned by using a software created by a researcher not involved in the study. The list generated by the algorithm was unavailable to authors.

Opaque envelopes containing the allocation group were sealed and sequentially numbered according to an electronically generated randomization list.

Data were electronically anonymized by using an individual alphanumeric code and analysed by investigators not involved in patient enrolment or data collection.

The trial was approved by the Institutional Ethics Committee of the University Hospital of Genoa on 9th April 2021.

After obtaining informed consent, eligible infants were randomly assigned to 1 of 2 study arms within 6 hours of birth: a treatment group or a control group.

5.4 Continuous glucose monitoring

Real-time Medtronic MiniMed MMT-7820WE Guardian Connect (Northridge, CA 91325 USA) professional continuous glucose monitors with Enlite sensors (Medtronic of Canada Ltd, Brampton, Ontario) were placed as early as possible after study enrolment, preferably within 6 hours of birth. The sensors were inserted in the lateral thigh and secured with clear adhesive dressing after adequate disinfection of the site.

The sensor (Enlite sensor) is minimally invasive, soft, flexible, and disposable. This device is about 1 mm-wide and 10 mm-long, and it is mounted through a hollow needle. Continuous measurements were recorded for the first 6 days of life.

Two minutes before the procedure, 0.5 mL of glucose 10% was administered to the patient to minimize pain associated with sensor insertion.

The CGM was calibrated using capillary blood glucose values measured by FreeStyle Optium Neo H glucometer (Abbott Healthcare, Massachusetts, USA).

Every 5 min, 24 h a day, the sensor detects interstitial fluid blood glucose and stores it in the device, providing 288 interstitial glucose values per day.

Glycaemic monitoring was performed at two different periods of preterm life:

- the first week of life.
- on the 32nd week of corrected age.

Obviously, each infant assigned to a specific study group remained in the same group during the second week of monitoring.

After completing 6 days of CGM, the neonatologist removed the sensor. The data were downloaded onto a Windows-based notebook computer running Medtronic Diabetes software.

In case of detachment or malfunction, the device was replaced no more than once. The system was removed if the patient needed to be transferred to another unit or hospital. The sensors were well tolerated in our babies without any complication.

5.4.1 Treatment group (Real time group)

This monitoring system gives clinicians "real time" glycaemic measurements.

Newborns assigned to the treatment group wore the CGM device with active alarms for hypoglycaemia (< 47 mg/dL) and hyperglycaemia (>180 mg/dL).

On admission we started parenteral nutrition with a glycemic rate intake (GIR) of 4-5 mg/kg/min in accordance with ESPGHAN guidelines[11].

In case of hypoglycaemia or hyperglycaemia, the glucose infusion rate was changed by the physician. The possibility of administering a bolus of 10% glucose solution was evaluated based on the ESPGHAN guidelines [11].

In case of hypoglycemia (< 47 mg/dl) or hyperglycemia (> 180 mg/dl), GIR was modified by the physicians needed, according to our internal protocol, in the same way as control group, with a substantial difference: if clinicians were informed that the blood glucose

trend was rising or falling, they could anticipate a hypo- or hyperglycemic episode by adjusting the GIR before the episode occurred. GIR adjustment was decided by the clinicians themselves. We decided to use insulin only in the case of persistent hyperglycemia despite a reduction in GIR.

5.4.2 Control group

Newborns assigned to the control group wore the CGM device with blinded monitor and no alarms. The monitor was placed inside a sealed envelope and connected to headphones that allowed not to hear the alarms.

Glucose infusion rate was adjusted based on blood glucose measurements performed every 3 hours in first day of life and, at minimum, every 8 hours the next days as is standard care at our department. On admission we started parenteral nutrition with a glycemic rate intake (GIR) of 4-5 mg/kg/min in accordance with ESPGHAN guidelines[11,75].

Glucose rate intake was adjusted based on blood glucose measurements performed every 3 hours in first day of life and every 8 hours the next days. In case of hypoglycemia (< 47 mg/dl) or hyperglycemia (> 180 mg/dl), GIR was modified by the physicians according to our internal protocol. When blood glucose was below 47 mg/dL or above 180 mg/dL GIR was adjusted by 0.5 mg/kg/min. In cases where blood glucose dropped below 25 mg/dL, a bolus of 10% glucose solution (2 mL/kg) was administered. We decided to use insulin only in the case of persistent hyperglycemia despite a reduction in GIR.

5.5 MRI Acquisition Parameters

MRI examinations were performed using a 3T scanner (Ingenia Cx, Philips, Best, The Netherlands) equipped with a 32-channel head coil. All neonates were fed prior to the examination to promote physiological sedation, and scans were conducted during natural sleep with spontaneous breathing. Throughout the entire procedure, vital signs were continuously monitored non-invasively.

The imaging protocol included conventional and advanced sequences: T1-weighted, T2-weighted, susceptibility-weighted imaging (SWI), DWI, and DTI. The latter were acquired using the following standard parameters: TR/TE: 3000/85 ms; echo train length: 51; voxel size: 1.5 × 1.5 × 2 mm; number of slices: 56; number of diffusion gradient directions: 64; b-values: 0 and 1000 s/mm²; reconstruction matrix: 144 × 144. When technically feasible, an additional DWI sequence with reversed phase-encoding (B0inv) was acquired using the same parameters to allow geometric distortion correction.

Newborns enrolled in the study underwent brain MRI at 33 weeks corrected gestational age, when clinically permissible, and subsequently at TEA.

5.6 Post-processing of DTI Images

DTI data processing was performed using two open-source software packages: MRtrix3 (v. 3.0.4) and FSL – FMRIB Software Library (v. 6.0.5.2). All images initially underwent a preliminary quality assessment to exclude datasets affected by motion artifacts, field distortions, or technical issues related to the sequence or scanner hardware. Only datasets free from significant alterations were converted to NIfTI format and included in subsequent analytical steps. The selected images were then subjected to a series of standardized corrections aimed at removing phase-encoding distortions, patient motion, and systematic noise. Specifically, in subjects with reversed phase-encoding B0

acquisitions, the *topup* function was applied to correct distortions arising from magnetic field inhomogeneities. In subjects without reversed B0 images, distortions were corrected by registering the T2-weighted image to the B0 image (linear transformation), followed by nonlinear registration of the B0 image to the T2-weighted reference in diffusion space. Correction of eddy-current–related artifacts was performed using the *eddy_correct* function, applied prior to anatomical registration in cases lacking reversed B0 acquisitions.

An automatic brain extraction step was subsequently performed using an external atlas adapted to the neonatal population, with the aim of removing non-brain tissues and isolating the cerebral parenchyma. Using the *dtifit* function, a diffusion tensor was then fitted at each voxel, and diffusion metrics such as FA, AD, MD, and RD were computed. Once the DTI maps were obtained, the FA map was used for group comparison through TBSS. This technique first requires alignment of each FA map to a common space; hence a neonatal template derived from the developing Human Connectome Project (dHCP) (https://github.com/BioMedIA/dhcp-structural-pipeline) was used for the study. This step is essential to ensure inter-subject comparability, as individual FA maps originate from different anatomical spaces. Alignment to the common space involved two stages:

• **Linear registration** performed using rigid transformations (translation and rotation), to correct global differences in position, orientation, and scale across images.

• **Nonlinear registration** enabling more accurate alignment by adapting each image to the morphological characteristics of the reference template, thereby compensating for local deformations related to brain curvature or individual anatomical variability.

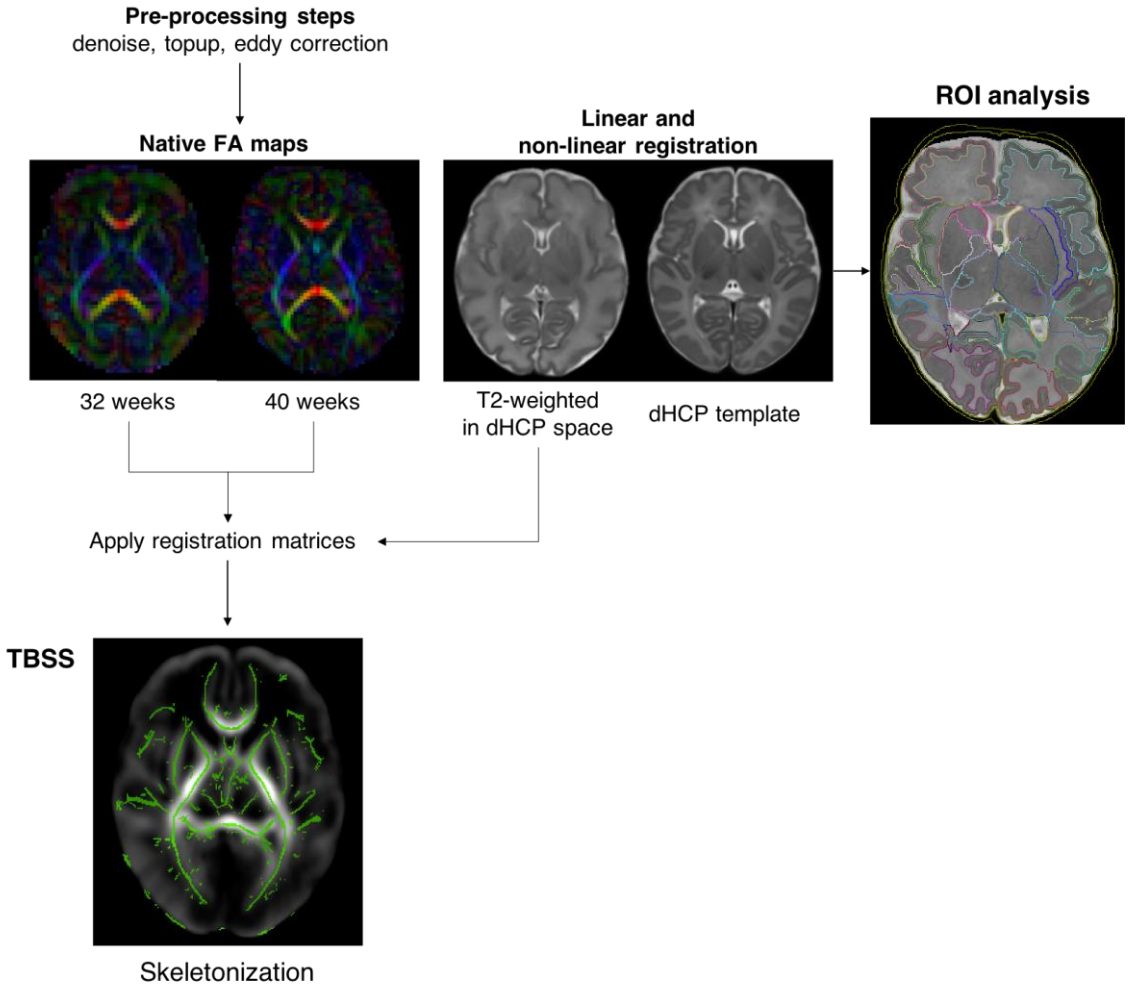

Figure 7. Workflow for the post-processing analysis. DTI images were acquired and subject to pre-processing steps. Linear and non-linear registration were applied to the generated DTI maps to transform images on common coordinates (dHCP template) to facilitate group-wise analysis. Structural brain volumes were calculated through ROI analysis using the dHCP structural pipeline for parcellization.

A mean FA map was then generated by averaging all individual FA maps, providing a synthetic representation of white-matter organization in the study cohort. A morphological thinning algorithm was applied to the mean FA map to obtain the "white-matter" skeleton. The skeletonization procedure provides a schematic representation of the central trajectories of major white-matter tracts, reducing spatial complexity and allows to focus the analysis on regions of highest directional anisotropy. Before statistical testing, a thresholding step (FA > 0.15) was applied to retain only voxels

with marked directional anisotropy, likely corresponding to well-organized white-matter bundles. The resulting skeletonized FA data were then used for statistical comparison between the two study groups.

In parallel with the TBSS analysis, a volumetric ROI-based analysis was conducted. Using pre-processed T2-weighted images and a neonatal-specific atlas, each subject was segmented into 87 anatomical regions, including cortical and deep gray matter as well as white-matter areas. For each ROI, a binary mask was generated, and its absolute volume was calculated, followed by normalization to total intracranial volume. The resulting volumetric measures were used for statistical comparison between groups to identify potential regional structural differences associated with the distinct glycemic management approaches.

5.7 Griffiths Scales of Child Development

We prospectively collected data from Griffiths Scales of Child Development (GMDS) (0-2 years) assessment performed at 24 months of correct age. GMDS yields five subscales: locomotor, personal–social, hearing and speech, eye and hand coordination, and performance. Each domain generates a standardized score, and a General Developmental Quotient (GDQ) is calculated by combining all subscale scores. The mean GDQ is 100 (SD ±12), with higher scores indicating better developmental performance. Cognitive outcome was classified as normal when GDQ was > 85, borderline when GDQ was from 70 to 85, and delayed when GDQ was lower than 70[76].

5.8 Outcomes

Primary outcomes were the number of hypo- and hyperglycaemic episodes and the occurrence of prolonged hypoglycaemia (>60 min) during the first week and at 32 weeks of corrected age. We also analysed several secondary outcomes. First, glycaemic variability, assessed by daily MAGE during the first week and weekly at 32 weeks. Second, the effect of CGM on cerebral white matter development in preterm neonates. DTI images acquired at 33 weeks and at term-equivalent age were processed, and TBSS was performed for FA and MD metrics. ROI analysis was also conducted at the corresponding time points on T2-weighted images to identify structural differences between the two study groups. Lastly, inter-group differences in psychomotor development at 24 months of corrected age were evaluated using the Griffiths Mental Development Scales.

5.9 Statistical analysis

The statistical analysis was conducted according to a predefined plan, with the aim of comparing the glycaemic profiles of preterm infants assigned to real-time continuous glucose monitoring versus those managed with standard care. Baseline characteristics of the two groups were summarised using descriptive statistics: mean and standard deviation or median and range for continuous variables, and absolute and relative frequencies for categorical variables. The distribution of continuous variables was assessed using the Kolmogorov–Smirnov test; when normality assumptions were not met, non-parametric tests were applied. Differences between groups were analysed using the Mann–Whitney

U test for continuous variables and the χ^2 test or Fisher's exact test for categorical variables.

The primary glycaemic endpoints — number of hypoglycaemic episodes (180 mg/dL), and duration of hypoglycaemic episodes lasting >60 minutes — were compared between groups using the same non-parametric approach, given the discrete and non-normally distributed nature of the data. Glycaemic variability was assessed using Standard Deviation (SD) and the Mean Amplitude of Glycaemic Excursions (MAGE), calculated using the EasyGV software from CGM data. For the first week of life, MAGE was calculated daily; at 32 weeks postmenstrual age, variability was assessed using the full week of CGM data for each infant.

CGM data were included in the analysis only when the daily trace was sufficiently complete to allow reliable computation of variability indices. Short interruptions due to transient sensor detachment or malfunction were not interpolated, whereas days with insufficient CGM data were excluded from variability analyses according to predefined criteria. To minimise bias related to incomplete glycaemic profiles, infants with less than 80% of the expected monitoring time were excluded from the analysis, as traces below this threshold were considered inadequate for accurate estimation of glycaemic variability metrics. Given the pilot nature of the study and the need for complete CGM datasets to compute the endpoints, analyses were performed using a per-protocol approach.

All analyses were conducted using SPSS (IBM SPSS Statistics, Chicago, IL). A two-tailed p value < 0.05 was considered statistically significant.

To analyze differences in white matter tracts obtained using TBSS, the two groups were compared using an independent samples t-test, with correction for type I error risk using the Family-Wise Error (FWE) rate. An uncorrected analysis was also performed for comparative purposes. The null distribution for statistical significance was estimated

using 500 permutations. A similar analysis was performed to evaluate longitudinal differences between the first and second MRIs within each group, using a paired t-test (with FWE correction and 500 permutations). In addition, an ROI analysis was completed using the structural pipeline developed by the dHCP. For each patient, T2-weighted images were segmented into 87 regions of white and gray matter. The volumes were then calculated and divided by the total intracranial volume of each patient.

6 RESULTS

	Real time group n=26	Control group n=27	Adjusted p value
Gestational age, weeks, Mean (SD)	29+2	29+1	0.77
CI 95% mean	26+0 – 31+0	26+4 - 30+6	
Birthweight, g (SD)	1289 ± 276	1217 ± 258	0.77
APGAR 1' (median, mode)	7 (4; 9)	6 (1; 8)	0.77
APGAR 5' (median, mode)	8 (7; 10)	8 (3; 10)	0.77
Male (%)	10 (38,5%)	11 (40.7%)	0.93
Received antenatal steroids more than 24 h before delivery (%)	20 (76.9%)	24 (88.9%)	0.77
Delivery mode			
Spontaneous vaginal delivery (%)	8 (30.8%)	8 (29.6%)	1.0
Caesarean section (%)	18 (69.2%)	11 (70.4%)	
Number of infants delivered			
Multiple (%)	5 (19.2%)	7 (25.9%)	0.85
Maternal chorioamnionitis (%)	3 (11.5%)	3 (7.4%)	0.85
Death	0	0	-
Sepsis (%)	5 (19.2%)	7 (25.9%)	0.85
Intraventricular hemorrhage (%)	1 (3.8%)	3 (11.1%)	0.85
Treatment for arteriosus ductus			0.77
Paracetamol (%)	8 (30.8%)	16 (59.3%)	
Surgery (%)	1 (3.8%)	0	
Necrotizing enterocolitis (%)	0	2 (7.4%)	0.85
Retinopathy of prematurity (%)	5 (19.2%)	7 (25.9%)	0.85
Bronchopulmonary dysplasia (%)	1 (3.8%)	4 (14.8%)	0.80
Number of EUGR (Extra Uterine Growth Restriction)	14 (54%)	11 (41%)	0.85

Table 1. Clinical characteristics and clinical complications of the enrolled subjects

Table 1 reports the characteristics and clinical complications of the newborns in the two groups. No statistically significant differences were observed between groups with respect to sex, gestational age, birth weight, mode of delivery, Apgar scores, maternal chorioamnionitis, sepsis, intraventricular haemorrhage, necrotizing enterocolitis, retinopathy of prematurity, bronchopulmonary dysplasia, or mortality.

Fifty-nine newborns met the eligibility criteria for the study. Parents of 4 infant declined participation. Two infants in the real-time CGM group were excluded from the analysis because they did not reach the predefined ≥80% CGM data completeness threshold. In one case, the sensor repeatedly malfunctioned despite repositioning attempts, resulting in an insufficient usable trace. In the other case, the sensor battery expired after approximately 96 hours, preventing acquisition of the required monitoring duration.

A total of 53 infants were therefore included [Figure 8], with 26 assigned to the real-time group and 27 to the control group.

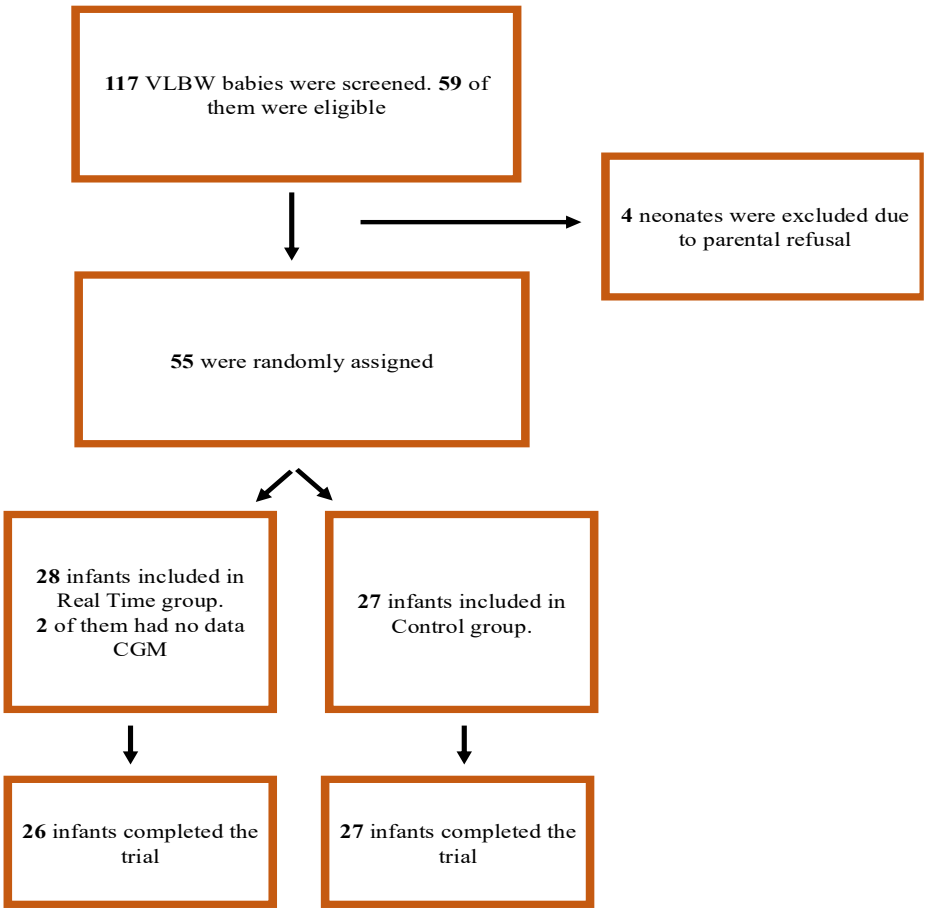

Figure 8. Design of the study

As shown in Table 2, the real-time group exhibited a significantly lower number of hypoglycaemic and hyperglycaemic episodes compared with the control group ($p < 0.001$).

A similar pattern was observed during the second week of monitoring ($p < 0.001$).

The real-time group also exhibited a reduced number of prolonged hypoglycaemic episodes, defined as episodes lasting more than 60 minutes.

Primary outcomes	Real time group n=26	Control group n=27	Adjusted p value
Number of episodes of Hypoglycemia (< 47 mg/dl)	339 (0.7%)	934 (1.8%)	<0.001
Number of episodes of hyperglycemia (> 180 mg/dl)	145 (0.3%)	830 (1.6%)	<0.001
Number of episodes of Hypoglycemia (< 47 mg/dl) on 32nd week of postmestrual age	260 (1.19%)	785 (2.9%)	<0.001
Number of episodes of hyperglycemia (> 180 mg/dl) on 32nd week of postmestrual age	1 (0.005%)	38 (0.14%)	<0.001
Episodes of Hypoglycemia> 60 minutes	5	28	0.049

Table 2. Comparison of hypoglycaemic and hyperglycaemic episodes between the real-time and control groups in the two weeks of monitoring

In cases of hypoglycaemia or hyperglycaemia, GIR were adjusted as needed by the physician. No infants required insulin. In the real-time CGM group, glucose administration was modified more frequently for both hypoglycaemic and hyperglycaemic events compared to the control group (Table 3).

Mean of changes of GIR per day in the first week of monitoring	Real time group n=26	Control group n=27	Adjusted p value
Day 1	3.92 ± 0.27	2.63 ± 0.49	< 0.01
Day 2	3.69 ± 1.09	2.52 ± 0.98	< 0.01
Day 3	3.04 ± 0.92	2.44 ± 0.80	0.01
Day 4	2.58 ± 1.47	2.22 ± 0.80	0.28
Day 5	2.62 ± 0.75	2.22 ± 0.70	0.04
Day 6	2.38 ± 0.64	2.22 ± 0.58	0.19
Mean of changes of GIR per day for hypoglycemic episodes in the first week of monitoring	**Real time group n=26**	**Control group n=27**	**Adjusted p value**
Day 1	2.35 ± 0.63	1.63 ± 0.57	< 0.01
Day 2	2.35 ± 0.69	1.48 ± 0.80	< 0.01
Day 3	1.73 ± 0.72	1.33 ± 0.78	0.07
Day 4	1.46 ± 0.70	1.26 ± 0.59	0.14
Day 5	1.38 ± 0.64	1.15 ± 0.53	0.12
Day 6	1.19 ± 0.69	1.19 ± 0.56	0.44
Mean of changes of GIR per day for hyperglycemic episodes in the first week of monitoring	**Real time group n=26**	**Control group n=27**	**Adjusted p value**
Day 1	1.58 ± 0.64	1.00 ± 0.56	< 0.01
Day 2	1.35 ± 0.69	1.04 ± 0.65	0.1
Day 3	1.31 ± 0.74	1.11 ± 0.93	0.25
Day 4	1.12 ± 1.14	0.96 ± 0.85	0.39
Day 5	1.23 ± 0.59	1.07 ± 0.68	0.25
Day 6	1.19 ± 0.69	1.04 ± 0.52	0.25

Table 3. Adjustments of glucose infusion rate (GIR) for hypoglycaemic and hyperglycaemic events in the real-time CGM and control groups.

The glycaemic variability, measured by the MAGE index (Table 4), revealed a significant difference in the first few days of life, with the real-time group showing lower variability, except on day 4. No statistically significant differences were observed on the Griffiths Scales (Table 5).

The MAGE trend in the first week of life for both groups is illustrated in Figure 9.

MAGE	**Real time group n=26**	**Control group n=27**	**Adjusted p value**
Day 1	5.87 ± 8.57 (mg/dl)	16.87 ± 9.16 (mg/dl)	0.03
Day 2	5.20 ± 6.04 (mg/dl)	20.00 ± 17.00 (mg/dl)	<0.01
Day 3	3.98 ± 5.09 (mg/dl)	16.21 ± 12.40 (mg/dl)	<0.01
Day 4	6.87 ± 6.95 (mg/dl)	11.60 ± 9.89 (mg/dl)	0.10
Day 5	7.59 ± 6.58 (mg/dl)	14.99 ± 5.73 (mg/dl)	<0.01
Day 6	10.02 ± 6.14 (mg/dl)	18.34 ± 7.78 (mg/dl)	0.04
MAGE on 32nd week of postmestrual age	**Real time group n=26**	**Control group n=27**	**Adjusted p value**
MAGE	14.88 ± 4.75 (mg/dl)	19.41 ± 8.39 (mg/dl)	0.01

Table 4. MAGE index to calculate glycaemic variability in the two groups.

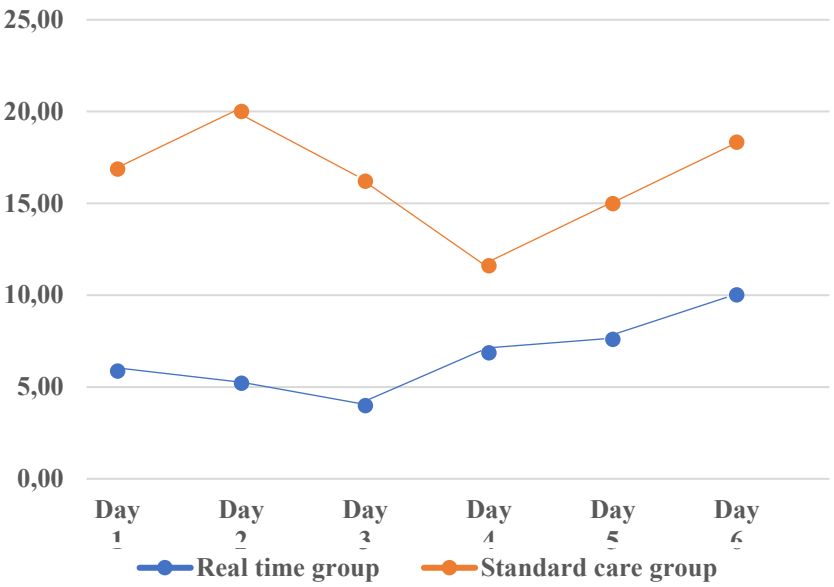

Figure 9. Trend of the MAGE index during the first week of glycaemic monitoring in the two study groups.

Griffiths at two years correct age (median, IQR)	Real time group n=26	Control group n=27	Adjusted p value
Total Score	90 (±2,74)	88 (±2,51)	0.68
Locomotor (A)	90 (±3.25)	92.5 (±2.88)	0.27
Personal Social (B)	95 (±2,56)	96 (±2,89)	0.27
Hearing and Speech (C)	91 (±2,99)	90 (±3,12)	0.34
Eye and Hand Coordination (D)	89(±1,87)	92 (±2,23)	0.47
Performance (E)	92 (±2,36)	89 (±2,89)	0.74

Table 5. Comparison of Griffiths Scores Between the Two Groups

Neuroimaging cohort

MRI analyses were performed on a reduced cohort selected from the original population, as only a subset of patients had brain MRI scans of adequate quality.

Variables		Cohort (n=29)	Real time group (n=10)	Control group (n=19)	p value
Sex	*M(%)*	14 (48)	4 (40)	10 (53)	0.70
	F(%)	15 (52)	6 (60)	9 (47)	
Delivery mode	*spontaneous (%)*	7 (24)	2 (20)	5 (26)	1
	caesarean (%)	22 (76)	8 (80)	14 (74)	
Centile	*Mdn*	72	68	72	0.91
	IQR	53	54	57	
Gestational age, weeks	*Mdn*	29	29	29	0.5
	IQR	3	3	3	
Birth weight, g	*Mdn*	1230	14450	1140	0.29
	IQR	560	513	530	
Recieved antenatal steriods	*Yes (%)*	25 (86)	9 (90)	16 (84)	1
	No (%)	4 (14)	1 (10)	3 (16)	
Maternal chorioamnioitis	*Yes (%)*	3 (10)	2 (20)	1 (5)	0.27
	No (%)	26 (90)	8 (80)	18 (95)	
Twin delivery	*Yes (%)*	10 (34)	3 (30	7 (37)	1
	No (%)	19 (66)	7 (70)	12 (63)	
APGAR 1'	*Mdn*	8	8	7.5	0.76
	Min;Max	4;9	4;9	5;8	
APGAR 5'	*Mdn*	9	8.5	9	0.5
	Min;Max	6;9	8;9	6;9	
Sepsi	*Yes (%)*	6 (21)	2 (20)	4 (21)	1
	No (%)	23 (79)	8 (80)	15 (79)	
Treatment for arteriosus ductus	*Paracetamol (%)*	15 (52)	8 (80)	7 (37)	0.05
	No (%)	14 (48)	2 (20)	12 (63)	
Retinopathy of prematurity	*Yes (%)*	6 (21)	0	6 (32)	0.07
	No (%)	23 (79)	10 (100)	13 (68)	
Bronchopulmonary dysplasia	*Yes (%)*	4 (14)	1 (10)	3 (16)	1
	No (%)	25 (86)	9 (90)	16 (84)	
Corrected Gestational age MRI I	*Mdn*	33	33	33	0.91
	IQR	1	0	2	
Corrected Gestational age MRII	*Mdn*	40	40	40	0.16
	IQR	1	0	1	
Interval between MRI scans, days	*Mdn*	49	49	48	0.26
	IQR	13	11	14	

Table 6. Characteristics of the cohort within the neuroimaging analysis

Assessment of white matter maturation through TBSS analysis

The TBSS analysis was performed to compare FA and MD values longitudinally, specifically at 33 and 40 weeks of age, and to examine differences in myelination and white matter development between groups. As expected, TBSS showed an increase in FA values for most tracts in the MRI scans acquired at TEA [Figure 10]. Conversely, MD values were higher in the initial scans, gradually reducing in the TEA imaging [Figure 11].

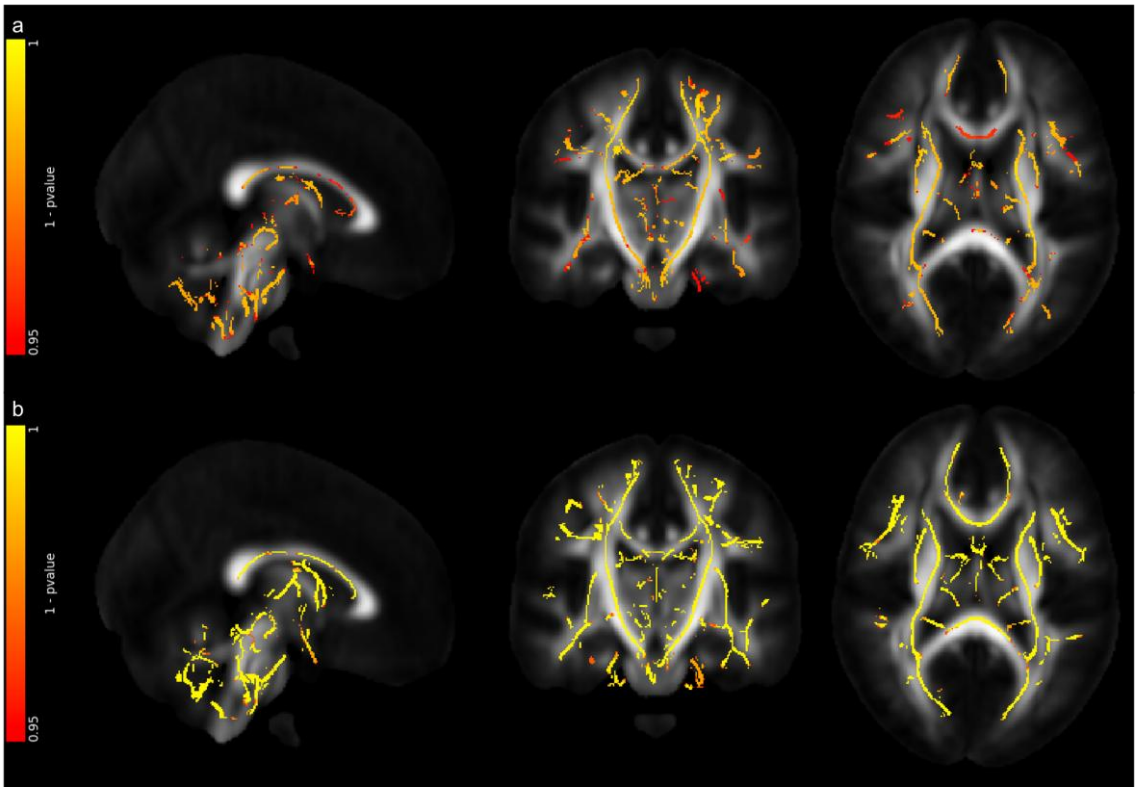

Figure 10. TBSS analysis comparing FA maps of MR imaging acquired at 33 and 40 weeks. Panels illustrate areas of higher values of FA in the 40-week MRI scan in the a) real time group and b) control group.

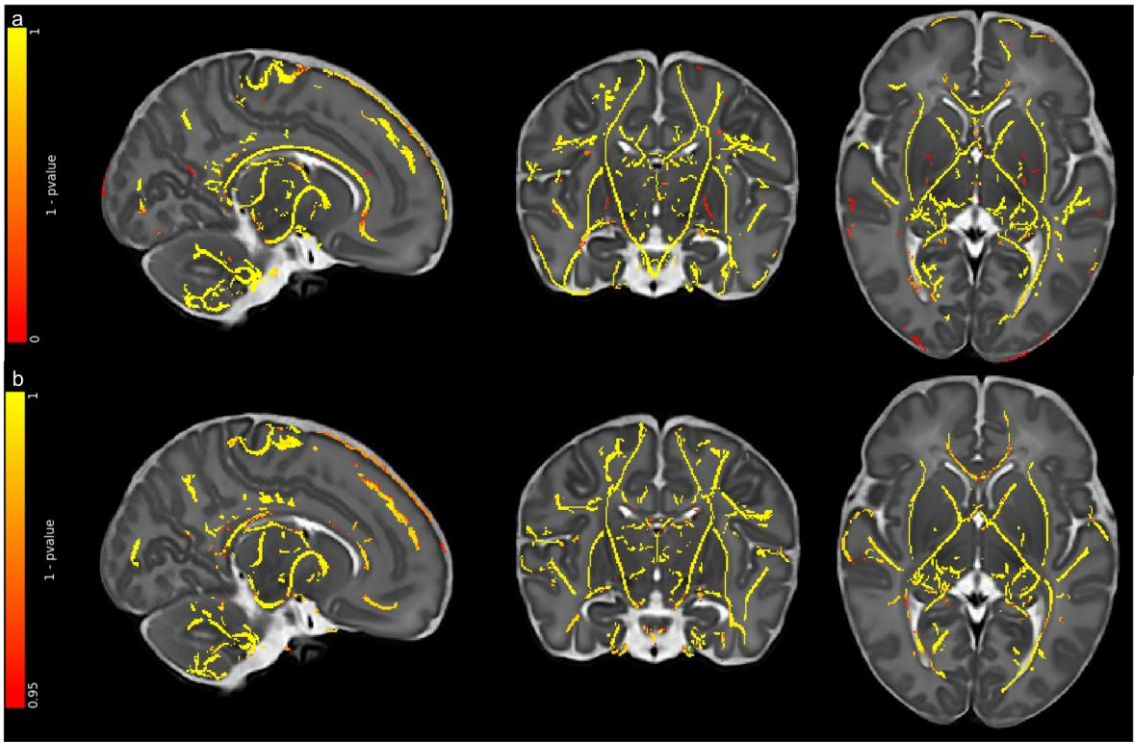

Figure 11. TBSS analysis comparing MD maps of MR imaging acquired at 33 and 40 weeks. Panels illustrate areas of higher values of MD in the 33-week MRI scan in the a) real time group and b) control group.

For intergroup analysis, TBSS showed no significant differences in FA or MD values between the real time and control group.

7. DISCUSSION

Preterm infants are notoriously vulnerable to metabolic alterations; among them, disorders affecting glycaemic metabolism are common[66,77,78].

This predisposition is due to the low activity of glucose-6-phosphatase, to their immature regulatory system, to insufficient glycogen stores, to the basal increase in glucose metabolism and to a limited capacity to access alternative energy sources[7,8,10]. Detection of hypoglycaemia is important because it is associated with increased morbidity and can result in seizures, impaired motor function and visual disturbances, among other effects[6].

Our study adds evidence to corroborate that continuous glycaemic monitoring is more effective than extemporaneous capillary sampling in maintaining euglycemia in preterm[73,78].

Previous studies in which CGM monitoring has been used have shown a higher rate of hypoglycaemia detection, confirming that hypoglycaemia is more frequent, and most of the time asymptomatic, in VLBW babies [79]. Furthermore, the use of CGMs in a real-time mode provided new possibilities into the management of hypoglycaemia, allowing them to be treated earlier and to reduce their duration [66].

In the recent past, Galderisi et al highlight how the use of the CGM and the modification of the GIR according to the CGM can lead to more time spent in euglycemia, minimizing glycaemic variability during the first days of life[73]

The same authors in a more recent Cochrane published in 2021 highlighted that there is limited evidence to determine whether CGM impacts the mortality or morbidity of preterm infants, suggesting how further studies are needed to understand whether its use may have long-term implications particularly in terms of neurodevelopmental impairments [78].

In accordance with the most recent literature, in our study we obtained a reduction in hypoglycaemic and hyperglycaemic episodes in the real time group. We also observed a reduction of long-lasting hypoglycaemic episodes (> 60 minutes) known to be even more harmful. Accordingly, episodes of severe and long-lasting hypoglycaemia are known to be associated with poor neurological outcome. [6,80,81].

Even more interesting, the number of hypoglycaemias and hyperglycaemias is also reduced in the real time group in the second week of monitoring (32nd week of postmenstrual age). Maybe, a better glycaemic control, even at a later stage of preterm life, could be related simply to the use of CGM as previously demonstrated or linked to the fact that better glycaemic control at birth may also improve glycaemic control in the long term. Tottman et al. investigated the correlation between tighter glycaemic control of hyperglycaemic preterm infants and short- and long-term outcomes, highlighting that this did not change survival or neurodevelopment. However, infants in the tight glucose control group had greater height-adjusted lean mass than those in the standard glucose control group and lower fasting glucose concentrations[82].

We compared changes in GIR based on glycemia measured by CGM in real-time group versus venipuncture (control group) to assess differences in clinical decisions. In the first week, especially during the first two days, GIR adjustments were significantly more frequent in the real-time group, maybe due to the possibility of adjusting the GIR not only in cases of hypo- or hyperglycemia, but also when a rising or falling trend was detected. This suggests that CGM data may influence early management more than conventional measurements. Despite more frequent changes in the glycaemic rate in the real time group, we did not observe an increase in EUGR (Extra Uterine Growth Restriction) compared to the control group (p value=0.9)[83,84]. While prolonged symptomatic neonatal hypoglycemia is clearly linked to brain injury, the impact of mild, asymptomatic

hypoglycemia and its relationship with neurodevelopment or hyperglycemia remains uncertain, with inconsistent evidence in the literature [67,81,85,86].

A randomized, controlled, longitudinal intervention study published in 2016 stratified preterm infants into four groups according to their glucose concentrations. Standardized cognitive, academic, and behavioural assessments were administered at 3, 8, and 18 years of age to compare developmental outcomes across groups. No significant differences in cognitive or academic performance were identified between the control group and those exposed to neonatal hypoglycaemia at any assessment point[89].

Conversely, a separate study reported that early transient neonatal hypoglycaemia was associated with lower achievement test scores at 10 years of age[90].

In our research, no statistically significant differences were observed in the Griffiths Developmental Scales scores at two years of corrected age. The sample size in our study was likely insufficient to detect differences in neurological outcomes. Consequently, larger, multicenter trials would be required to more comprehensively investigate this issue.

We assessed CGM effectiveness in reducing glycemic variability using the MAGE index, evaluating subjects during the first six days of life and again at 32 weeks postmenstrual age—unlike previous studies. MAGE index is a key index for intraday glycemic variability as it is independent of mean glucose and focuses on major swings[74]. It was calculated as the mean of the absolute differences between consecutive peaks and nadirs of glucose excursions exceeding one standard deviation from the mean glucose value, using continuous glucose monitoring data. Higher MAGE indicates greater variability and metabolic stress, while lower values reflect more stable control and reduced risk of complications. Using the MAGE index, we found lower glycemic variability in the real-time group during the first six days, with significant improvement also in the second

week. Unlike previous studies, our data show that CGM reduces hypo/hyperglycemic episodes and variability not only in early life but also in subsequent weeks.

Data on glycemic variability and outcomes in preterm infants are scarce, though in diabetes increased variability is linked to oxidative stress and adverse cognitive outcomes. Poorly controlled diabetes doubles the risk of cognitive impairment and triples dementia progression, especially with systemic inflammation. [87,88]. Few studies, including ours, show that CGM can reduce glycemic variability in neonates, potentially mitigating oxidative stress [73].

Metabolic pathways regulate neurodevelopment through processes like signaling, differentiation, and proliferation. Brain glucose metabolism is key to astrocyte–oligodendrocyte interactions for myelin formation and white matter development yet translating these mechanisms into neuroprotective strategies beyond severe hypoglycemia remains challenging. Despite evidence of white matter vulnerability to oxidative stress in preterm infants (28–29 weeks), studies on neonatal glucose control are scarce. Maintaining glucose homeostasis during this critical period may be pivotal. The absence of neurodevelopmental differences between CGM and control groups likely reflects limited follow-up duration.

To further explore how improved glycaemic stability might influence early brain maturation, we examined the structural development of white matter in our cohort. We conducted a qualitative assessment of their magnetic resonance imaging scans to identify potential differences associated with tighter glucose control.

Regarding the MRI analysis, we observed higher FA values at term-equivalent age and higher MD values in the early MRI scans. These findings are in line with previously published literature[45,52] and reflect the expected developmental differences in brain maturation and white matter microstructure across these time points. FA typically

increases and MD decreases as myelination progresses and fibre organization becomes more coherent, which supports the internal consistency of our data. However, when comparing the two study groups, we did not detect significant differences in either FA or MD at either the early or the term-equivalent MRI assessment. This lack of detectable group differences may be attributable to the limited sample size available for diffusion analysis, which reduces statistical power and may mask subtle microstructural alterations. Larger cohorts or longitudinal designs might be necessary to clarify whether more nuanced differences in white matter development exist between the groups.

8 LIMITATIONS OF THE STUDY

The principal limitation of this study lies in its limited sample size, which is particularly evident in the small number of infants who underwent MRI at 33 weeks of corrected age. This constraint substantially reduces the ability to detect statistically or clinically meaningful differences within such a restricted cohort.

Furthermore, regarding glycaemic measurements, it is not possible to definitively exclude the presence of measurement bias related to the inherent sampling delay (with data acquired every five minutes) or potential issues concerning sensor calibration. Moreover, although standard thresholds are commonly employed to define hypo- and hyperglycaemia in neonates, current evidence remains insufficient to determine which specific values truly correspond to differences of clinical relevance.

9 CONCLUSIONS

Early life is critical for neurodevelopment and long-term metabolic health, and glycemic variability may play an important role. In recent years, scientific research has increasingly highlighted the critical role of the first days and weeks of an infant's life, with particular emphasis on how metabolic balance and nutrition influence neurological development and the long-term risk of metabolic syndrome. Our study shows CGM reduces hypo and hyperglycemic episodes and improves glucose stability in preterm infants. While MAGE is widely used to assess variability in diabetes, its application in neonates may be suboptimal due to different metabolic characteristics. Limitations include small sample size and scarce comparative data, underscoring the need for larger multicenter trials to validate these findings and optimize glycemic control in this vulnerable population[89,90].

In conclusion, our findings underscore the potential of CGM as an essential tool in optimizing glucose management, improving health outcomes in premature infants, and supporting the broader goal of promoting healthy metabolic development in early life.

10 STATEMENT OF ETHICS

This study was conducted in accordance with the Declaration of Helsinki and approved by the Ethics Committee of Liguria Region (protocol 277/2021, date of approval 6 September 2021). Written informed consent was obtained from the participant's parent/legal guardian/next of kin prior to participate in the study

11 CONFLICTS OF INTEREST STATEMENT

The authors have no conflicts of interest to declare.

12 REFERENCES

1. Phillips, C., Velji, Z., Hanly, C. & Metcalfe, A. Risk of recurrent spontaneous preterm birth: A systematic review and meta-analysis. *BMJ Open* vol. 7 Preprint at https://doi.org/10.1136/bmjopen-2016-015402 (2017).

2. Blencowe, H. *et al.* National, regional, and worldwide estimates of preterm birth rates in the year 2010 with time trends since 1990 for selected countries: A systematic analysis and implications. *The Lancet* **379**, 2162–2172 (2012).

3. Liu, L. *et al.* Global, regional, and national causes of child mortality: an updated systematic analysis for 2010 with time trends since 2000. *The Lancet* **379**, 2151–2161 (2012).

4. Thompson-Branch, A. & Havranek, T. *Neonatal Hypoglycemia Education Gap*. http://pedsinreview.aappublications.org/.

5. Musso, V. *et al.* Continuous Glucose Monitoring in Preterm Infants: The Role of Nutritional Management in Minimizing Glycemic Variability. *Antioxidants* **11**, (2022).

6. De Angelis, L. C. *et al.* Neonatal Hypoglycemia and Brain Vulnerability. *Frontiers in Endocrinology* vol. 12 Preprint at https://doi.org/10.3389/fendo.2021.634305 (2021).

7. Girard J. Gluconeogenesis in late fetal and early neonatal life. *Biol Neonate* (1986).

8. Mitanchez, D. Glucose regulation in preterm newborn infants. *Hormone Research* vol. 68 265–271 Preprint at https://doi.org/10.1159/000104174 (2007).

9. Hoseth, E., Joergensen, A., Ebbesen, F. & Moeller, M. *Blood Glucose Levels in a Population of Healthy, Breast Fed, Term Infants of Appropriate Size for Gestational Age*. http://fn.bmj.com/.

10. Hume, R., Burchell, A. & Burchel, A. *Abnormal Expression of Glucose-6-Phosphatase in Preterm Infants*. *Archives ofDisease in Childhood* vol. 68 (1993).

11. Mesotten, D. *et al.* ESPGHAN/ESPEN/ESPR/CSPEN guidelines on pediatric parenteral nutrition: Carbohydrates. *Clinical Nutrition* **37**, 2337–2343 (2018).

12. Kalhan, S., Peter-Wohl, S. & Schwartz, R. *HYPOGLYCEMIA: WHAT IS IT FOR THE NEONATE? AMERICAN JOURNAL OF PERINATOLOGY* vol. 17 (2000).

13. Adamkin, D. H. *et al.* Clinical report - Postnatal glucose homeostasis in late-preterm and term infants. *Pediatrics* **127**, 575–579 (2011).

14. Beardsall, K., Ogilvy-Stuart, A. L., Ahluwalia, J., Thompson, M. & Dunger, D. B. The continuous glucose monitoring sensor in neonatal intensive care. *Arch. Dis. Child. Fetal Neonatal Ed.* **90**, (2005).

15. Beardsall, K. *et al. Early Insulin Therapy in Very-Low-Birth-Weight Infants*. *n engl j med* vol. 18 www.nejm.org (2008).

16. Hays, S. P., Smith, E. O. B. & Sunehag, A. L. Hyperglycemia is a risk factor for early death and morbidity in extremely low birth-weight infants. *Pediatrics* vol. 118 1811–1818 Preprint at https://doi.org/10.1542/peds.2006-0628 (2006).

17. Beardsall, K. *et al.* Real-time continuous glucose monitoring in preterm infants (REACT): an international, open-label, randomised controlled trial. *Lancet Child Adolesc. Health* **5**, 265–273 (2021).

18. Kalhan, S. & Parimi, P. Gluconeogenesis in the fetus and neonate. *Semin. Perinatol.* **24**, 94–106 (2000).

19. Alsaleem, M., Saadeh, L. & Kamat, D. Neonatal Hypoglycemia: A Review. *Clinical Pediatrics* vol. 58 1381–1386 Preprint at https://doi.org/10.1177/0009922819875540 (2019).

20. Ziya Aral,' Kivilcim Gucuyener,', Y. *et al. Role of Excitatory Aminoacids in Neonatal Hypoglycemia*. *Acta Paediatrica Japonica* vol. 40.

21. Sang, W. S., Gum, E. T., Hamby, A. M., Chan, P. H. & Swanson, R. A. Hypoglycemic neuronal death is triggered by glucose reperfusion and activation of neuronal NADPH oxidase. *Journal of Clinical Investigation* **117**, 910–918 (2007).

22. Won Suh, S., Garnier, P., Aoyama, K., Chen, Y. & Swanson, R. A. Zinc release contributes to hypoglycemia-induced neuronal death. *Neurobiol. Dis.* **16**, 538–545 (2004).

23. Sensi, S. L. *et al.* The neurophysiology and pathology of brain zinc. *Journal of Neuroscience* **31**, 16076–16085 (2011).

24. Auer, R. N. Progress review: Hypoglycemic brain damage. *Stroke* **17**, 699–708 (1986).

25. Paudel, N. *et al.* Neonatal Hypoglycaemia and Visual Development: A Review. *Neonatology* vol. 112 47–52 Preprint at https://doi.org/10.1159/000456705 (2017).

26. Sannia, A. *et al.* Different gestational ages and changing vulnerability of the premature brain. *Journal of Maternal-Fetal and Neonatal Medicine* **28**, 2268–2272 (2015).

27. Ramenghi, L. A. *et al.* Germinal matrix hemorrhage: Intraventricular hemorrhage in very-low-birth-weight infants: The independent role of inherited thrombophilia. *Stroke* **42**, 1889–1893 (2011).

28. Rutherford, M. A. *et al.* Magnetic resonance imaging of white matter diseases of prematurity. *Neuroradiology* vol. 52 505–521 Preprint at https://doi.org/10.1007/s00234-010-0700-y (2010).

29. Volpe, J. J. Brain injury in premature infants: a complex amalgam of destructive and developmental disturbances. *The Lancet Neurology* vol. 8 110–124 Preprint at https://doi.org/10.1016/S1474-4422(08)70294-1 (2009).

30. Ariadne M & Linda S. de Vries. Parenchymal Brain Injury in the Preterm Infant: Comparison of Cranial Ultrasound, MRI and Neurodevelopmental Outcome. *Neuropediatrics* 80–89 (2001).

31. Bassi, L. *et al. Diffusion Tensor Imaging in Preterm Infants With Punctate White Matter Lesions*. (2011).

32. Nowell, M. A. *et al.* Immature brain: spin-echo pulse sequence parameters for high-contrast MR imaging. *Radiology* **162**, 272–273 (1987).

33. Triulzi, F., Baldoli, C. & Parazzini, C. Neonatal MR imaging. *Magn. Reson. Imaging Clin. N. Am.* **9**, 57–82, viii (2001).

34. Hinojosa-Rodríguez, M. *et al.* Clinical neuroimaging in the preterm infant: Diagnosis and prognosis. *Neuroimage Clin.* **16**, 355–368 (2017).

35. Dubois, J. *et al.* <scp>MRI</scp> of the Neonatal Brain: A Review of Methodological Challenges and Neuroscientific Advances. *Journal of Magnetic Resonance Imaging* **53**, 1318–1343 (2021).

36. Bhutta, A. T., Cleves, M. A., Casey, P. H., Cradock, M. M. & Anand, K. J. S. Cognitive and Behavioral Outcomes of School-Aged Children Who Were Born Preterm. *JAMA* **288**, 728 (2002).

37. Barkovich, A. J. Concepts of myelin and myelination in neuroradiology. *AJNR Am. J. Neuroradiol.* **21**, 1099–109 (2000).

38. Barkovich, A. J., Kjos, B. O., Jackson, D. E. & Norman, D. Normal maturation of the neonatal and infant brain: MR imaging at 1.5 T. *Radiology* **166**, 173–180 (1988).

39. Knickmeyer, R. C. *et al.* A Structural MRI Study of Human Brain Development from Birth to 2 Years. *The Journal of Neuroscience* **28**, 12176–12182 (2008).

40. Biswal, B., Zerrin Yetkin, F., Haughton, V. M. & Hyde, J. S. Functional connectivity in the motor cortex of resting human brain using echo-planar mri. *Magn. Reson. Med.* **34**, 537–541 (1995).

41. Neil, J. J. Diffusion imaging concepts for clinicians. *Journal of Magnetic Resonance Imaging* **27**, 1–7 (2008).

42. Le Bihan, D. *et al.* Diffusion tensor imaging: Concepts and applications. *Journal of Magnetic Resonance Imaging* **13**, 534–546 (2001).

43. Hagmann, P. *et al.* Understanding Diffusion MR Imaging Techniques: From Scalar Diffusion-weighted Imaging to Diffusion Tensor Imaging and Beyond. *RadioGraphics* **26**, S205–S223 (2006).

44. Soares, J. M., Marques, P., Alves, V. & Sousa, N. A hitchhiker's guide to diffusion tensor imaging. *Front. Neurosci.* **7**, (2013).

45. Chenevert, T. L., Brunberg, J. A. & Pipe, J. G. Anisotropic diffusion in human white matter: demonstration with MR techniques in vivo. *Radiology* **177**, 401–405 (1990).

46. Martinez-Heras, E., Grussu, F., Prados, F., Solana, E. & Llufriu, S. Diffusion-Weighted Imaging: Recent Advances and Applications. *Seminars in Ultrasound, CT and MRI* **42**, 490–506 (2021).

47. Tournier, J., Mori, S. & Leemans, A. Diffusion tensor imaging and beyond. *Magn. Reson. Med.* **65**, 1532–1556 (2011).

48. Mori, S., Crain, B. J., Chacko, V. P. & van Zijl, P. C. Three-dimensional tracking of axonal projections in the brain by magnetic resonance imaging. *Ann. Neurol.* **45**, 265–9 (1999).

49. Kindlmann, G. & Westin, C. Diffusion Tensor Visualization with Glyph Packing. *IEEE Trans. Vis. Comput. Graph.* **12**, 1329–1336 (2006).

50. Papadakis, N. G., Smponias, T., Berwick, J. & Mayhew, J. E. W. *k* -space correction of eddy-current-induced distortions in diffusion-weighted echo-planar imaging. *Magn. Reson. Med.* **53**, 1103–1111 (2005).

51. Hajnal, J. V. *et al.* MR Imaging of Anisotropically Restricted Diffusion of Water in the Nervous System. *J. Comput. Assist. Tomogr.* **15**, 1–18 (1991).

52. Hüppi, P. S. & Dubois, J. Diffusion tensor imaging of brain development. *Semin. Fetal Neonatal Med.* **11**, 489–497 (2006).

53. Huang, H. *et al.* White and gray matter development in human fetal, newborn and pediatric brains. *Neuroimage* **33**, 27–38 (2006).

54. CASCIO, C. J., GERIG, G. & PIVEN, J. Diffusion Tensor Imaging. *J. Am. Acad. Child Adolesc. Psychiatry* **46**, 213–223 (2007).

55. Brockstedt, S. *et al.* Triggering in Quantitative Diffusion Imaging with Single-Shot EPI. *Acta radiol.* **40**, 263–269 (1999).

56. Song, S.-K. *et al.* Dysmyelination Revealed through MRI as Increased Radial (but Unchanged Axial) Diffusion of Water. *Neuroimage* **17**, 1429–1436 (2002).

57. Snook, L., Plewes, C. & Beaulieu, C. Voxel based versus region of interest analysis in diffusion tensor imaging of neurodevelopment. *Neuroimage* **34**, 243–252 (2007).

58. Bodammer, N., Kaufmann, J., Kanowski, M. & Tempelmann, C. Eddy current correction in diffusion-weighted imaging using pairs of images acquired with opposite diffusion gradient polarity. *Magn. Reson. Med.* **51**, 188–193 (2004).

59. Rohde, G. K., Barnett, A. S., Basser, P. J., Marenco, S. & Pierpaoli, C. Comprehensive approach for correction of motion and distortion in diffusion-weighted MRI. *Magn. Reson. Med.* **51**, 103–114 (2004).

60. Clark, C. A., Barker, G. J. & Tofts, P. S. An in Vivo Evaluation of the Effects of Local Magnetic Susceptibility-Induced Gradients on Water Diffusion Measurements in Human Brain. *Journal of Magnetic Resonance* **141**, 52–61 (1999).

61. Zhou, Y. *et al.* A primary study of diffusion tensor imaging-based histogram analysis in vascular cognitive impairment with no dementia. *Clin. Neurol. Neurosurg.* **113**, 92–97 (2011).

62. Smith, S. M. *et al.* Tract-based spatial statistics: Voxelwise analysis of multi-subject diffusion data. *Neuroimage* **31**, 1487–1505 (2006).

63. Di Paola, M. *et al.* When, where, and how the corpus callosum changes in MCI and AD. *Neurology* **74**, 1136–1142 (2010).

64. Ranger, M. *et al.* Neonatal Pain-Related Stress Predicts Cortical Thickness at Age 7 Years in Children Born Very Preterm. *PLoS One* **8**, (2013).

65. Montaldo, P. *et al.* Continuous glucose monitoring profile during therapeutic hypothermia in encephalopathic infants with unfavorable outcome. *Pediatr. Res.* **88**, 218–224 (2020).

66. Uettwiller, F. *et al.* Real-time continuous glucose monitoring reduces the duration of hypoglycemia episodes: A randomized trial in very low birth weight neonates. *PLoS One* **10**, (2015).

67. McKinlay, C. J. D. *et al.* Neonatal Glycemia and Neurodevelopmental Outcomes at 2 Years. *New England Journal of Medicine* **373**, 1507–1518 (2015).

68. McKinlay, C. J. D. *et al.* Continuous glucose monitoring in neonates: a review. *Matern. Health Neonatol. Perinatol.* **3**, (2017).

69. Monnier, L. *et al. Activation of Oxidative Stress by Acute Glucose Fluctuations Compared With Sustained Chronic Hyperglycemia in Patients With Type 2 Diabetes*. *JAMA* vol. 295 www.jama.com (2006).

70. Ozsurekci, Y. & Aykac, K. Oxidative Stress Related Diseases in Newborns. *Oxidative Medicine and Cellular Longevity* vol. 2016 Preprint at https://doi.org/10.1155/2016/2768365 (2016).

71. Jagła, M. *et al.* Defining Glycemic Variability in Very Low-Birthweight Infants: Data from a Continuous Glucose Monitoring System. *Diabetes Technol. Ther.* **20**, 725–730 (2018).

72. Szymońska, I., Jagła, M., Starzec, K. & Kwinta, P. Glycemic variability in continuous glucose monitoring negatively correlates with gestational age in very low birth weight infants. *Journal of Maternal-Fetal and Neonatal Medicine* **33**, 3041–3043 (2020).

73. Galderisi, A. *et al. Continuous Glucose Monitoring in Very Preterm Infants: A Randomized Controlled Trial*. http://pediatrics.aappublications.org/.

74. Monnier, L., Colette, C. & Owens, D. R. *Glycemic Variability: The Third Component of the Dysglycemia in Diabetes. Is It Important? How to Measure It? Journal of Diabetes Science and Technology* vol. 2 www.journalofdst.org (2008).

75. Mesotten, D. *et al.* ESPGHAN/ESPEN/ESPR/CSPEN guidelines on pediatric parenteral nutrition: Carbohydrates. *Clinical Nutrition* **37**, 2337–2343 (2018).

76. Green E, SL, BS, CJ, FC, HK, LH, MR, MC, MP, OR, PR, & VD. Griffiths III: Griffiths Scales of Child Development, Third Edition. Hogrefe Ltd; 2016.

77. Bonet, J. *et al.* Continuous Glucose Monitoring among Infants Born Very Preterm: Evidence for Accuracy in Neonatal Intensive Care. *J. Pediatr.* 114416 (2024) doi:10.1016/j.jpeds.2024.114416.

78. Galderisi, A., Trevisanuto, D., Russo, C., Hall, R. & Bruschettini, M. Continuous glucose monitoring for the prevention of morbidity and mortality in preterm infants. *Cochrane Database of Systematic Reviews* vol. 2021 Preprint at https://doi.org/10.1002/14651858.CD013309.pub3 (2021).

79. Platas, I. I. *et al.* Continuous glucose monitoring in infants of very low birth weight. *Neonatology* **95**, 217–223 (2009).

80. Shah, R., Harding, J., Brown, J. & Mckinlay, C. Neonatal Glycaemia and Neurodevelopmental Outcomes: A Systematic Review and Meta-Analysis. *Neonatology* vol. 115 116–126 Preprint at https://doi.org/10.1159/000492859 (2019).

81. Kaiser, J. R. *et al.* Association between transient newborn hypoglycemia and fourth-grade achievement test proficiency: A population-based study. *JAMA Pediatr.* **169**, 913–921 (2015).

82. Tottman, A. C. *et al.* Long-Term Outcomes of Hyperglycemic Preterm Infants Randomized to Tight Glycemic Control. *Journal of Pediatrics* **193**, 68-75.e1 (2018).

83. Makker, K., Ji, Y., Hong, X. & Wang, X. Antenatal and neonatal factors contributing to extra uterine growth failure (EUGR) among preterm infants in Boston Birth Cohort (BBC). *Journal of Perinatology* **41**, 1025–1032 (2021).

84. Maiocco, G. *et al.* Evaluation of Extrauterine Head Growth From 14-21 days to Discharge With Longitudinal Intergrowth-21st Charts: A New Approach to Identify Very Preterm Infants at Risk of Long-Term Neurodevelopmental Impairment. *Front. Pediatr.* **8**, (2020).

85. McKinlay, C. J. D. *et al.* Association of neonatal glycemia with neurodevelopmental outcomes at 4.5 years. *JAMA Pediatr.* **171**, 972–983 (2017).

86. Burns, C. M., Rutherford, M. A., Boardman, J. P. & Cowan, F. M. Patterns of cerebral injury and neurodevelopmental outcomes after symptomatic neonatal hypoglycemia. *Pediatrics* **122**, 65–74 (2008).

87. Dove, A. *et al.* The impact of diabetes on cognitive impairment and its progression to dementia. *Alzheimer's and Dementia* **17**, 1769–1778 (2021).

88. Panfoli, I. *et al.* Oxidative stress as a primary risk factor for brain damage in preterm newborns. *Frontiers in Pediatrics* vol. 6 Preprint at https://doi.org/10.3389/fped.2018.00369 (2018).

89. Zhou, Y. & Xu, Y. Nutrition and Metabolism in the First 1000 Days of Life. *Nutrients* vol. 15 Preprint at https://doi.org/10.3390/nu15112554 (2023).

90. Koletzko, B. *et al.* The power of programming and the earlynutrition project: Opportunities for health promotion by nutrition during the first thousand days of life and beyond. *Ann. Nutr. Metab.* **64**, 187–196 (2014).